FERMILAB-TM-2116   June 2000

Search for a C0 IR Design Using Existing Magnets

John A. Johnstone
Fermi National Accelerator Laboratory

February 29, 2000

Abstract

Future upgrades at Fermilab possibly include installation of a third detector in the Tevatron at the C0 straight section. The front-running contender for this site is currently the BTeV heavy quark program. A significant fraction of proposed BTeV detector R&D calls for installation of a new low–luminosity interaction region at C0 early in Run II. New magnets will not be available during the interim period and any 'medium' β^* IR insert must therefore be designed solely from Tevatron spares. This paper discusses some of the IR optics design issues related specifically to this magnet restriction and, more generally, issues affecting the Tevatron and its operation that will arise with the installation of any low–β^* IR at C0. The results of several attempts (& subsequent failures) to find a viable C0 IR optics solution using existing magnets are presented.

CONTENTS

1. INTRODUCTION

It has been proposed that at some point in the future a third detector will be installed in the Tevatron, at the C0 straight section, forming the foundation of a dedicated bottom-quark physics program at the collider. BTeV has devised a phased plan for development of a C0 detector. In this scheme the IR collision optics would be continually upgraded and refined through a series of developmental stages, culminating ultimately in a true low β^* (~0.35 m) IP, comparable to the two existing IP's.

The first step in this R&D program calls for design and installation of an intermediate–β^* (< 5 m) collision region fairly early in Run II. There are no new magnets available for this stage & so it is a considerably more formidable challenge than starting with a blank sheet of paper to design the final low–β insert. Section 2 outlines other constraints imposed on Phase One of the IR design. Various attempts to create a satisfactory medium–β^* IR are the subjects of Section 3 & Section 4. The reasons for their failure are examined in Section 5. For Section 6, the notion of a 'medium'–β^* IR is abandoned, and some possibilities are explored for creating colliding beams in the regular high–β optics of the C0 Collins insert. Finally, Section 7 reiterates the few lessons learned in this study -- the most difficult design obstacles encountered that <u>will</u> reappear in any future C0 IR design.

2. C0 IR DESIGN RESTRICTIONS

A Memorandum of Understanding, reached between Fermilab & BTeV [1] outlines the boundary conditions for developing a C0 IR design. Phase One of this BTeV R&D project calls for design of a medium β^* IR insert which realizes the following objectives:

" (1) specification of the magnets to be used (magnets will be chosen from existing magnets [2]);
(2) specification of separators (number & positions - design will be unchanged);
(3) specification of the correction scheme (steering corrections & any higher order corrections that might be required), and;
(4) longitudinal layout of insertion. (... The intent is to design an insertion that is sufficiently flexible that it can work in a variety of scenarios...).... "

The Memorandum outlines a second phase of developmental goals, calling for a series of insertion upgrade designs (including new magnets), resulting eventually in an IR insert with $\beta^* \approx 35$ cm.

The BTeV & Tevatron groups added additional constraints to the MOU list:

(5) magnets must not encroach upon the detector space 45' both sides of the IP;
(6) the synch light monitor will be located at B48;
(7) $\eta^* = \eta'^* = 0$ at B0 & D0, as in the Run II lattice;
(8) dispersion < 8 m in the arcs;
(9) β-wave < ±2 % in the arcs;
(10) operating scenarios should cover 3 IP's at collision, any 2 IP's, and any single IP, and;
(11) tunes are to remain fixed at (20.585, 20.575), as in the Run I & II lattices.

The first 6 items reflect physical constraints on the insert design, while (7)–(11) are optical constraints, primarily insisting that adding a C0 IR must not disrupt standard Tevatron operations.

2.1. IR Optics Complications

The maximum gradients of the available spare magnets are roughly 60% that of the B0 & D0 triplet quads (17.155 T/m/kA *cf* 29.018 T/m/kA); the only exceptions being the high-field 55" quads removed from the Q1 positions at B0 & D0 for Run II. The spares inventory includes neither the high-gradient quads from the original Tevatron low-beta inserts nor any spares for the current IR

[1] Memorandum of Understanding, E897, BTeV R&D Project, November, 1998.
[2] A menu of the available magnets is provided in Appendix I.

triplets. The paucity of free space further exacerbates design problems. The restriction that nothing encroaches upon the 45' of space reserved for the BTeV detector each side of the IP pushes the first low-beta magnets nearly twice as far away from the IP than the corresponding final focus quads at B0 & D0. With these constraints a doublet approach to a low-β solution at C0 is the only possible option -- there simply is not sufficient room to accommodate a triplet plus the necessary separators.

The principal argument for using triplets at B0 & D0 is to keep β_{max} as small as possible, which is most efficiently accomplished by triplet focusing. A doublet design does have advantages over a triplet principally in that it occupies less space and requires lower gradients. However, the one glaring disadvantage is that β_{max} is ~3 – 4 times larger for a given β^* than it would become in a triplet. Consequently, the minimum operational β^* might well be determined by the aperture of the low-beta quadrupoles rather than the maximum attainable magnet gradients.

In Run II the Tevatron operates with tunes near the half-integer, at (μ_x, μ_y) = (20.585, 20.575). The addition of a 3rd IR to the Tevatron will, if left uncorrected, raise the tunes by roughly a half-integer, placing them right onto the integer resonance at 21.0. This extra half integer must be added or subtracted somewhere in the ring to retrieve the original fractional tune operating point. Furthermore, this must be accomplished in such a way that neither destroys the optics & head-on collisions at B0 & D0 nor degrades beam separation in the arcs.

3. INDEPENDENT ARC QUADRUPOLES

There is $116^1/_2$' of space between the C0 IP and the first arc dipole. The BTeV detector occupies 45' of this space & three separators plus their ancillary hardware fills up another $33^1/_2$'. This leaves just 38' of room for the doublet focusing elements. The earliest attempts to design a medium-β^* insert relied on individually-powering and/or replacing the standard 66" arc quadrupoles to match the IP optics into the standard arc values. Outlines of two such attempts (2 out of many similar models) are described in the following sections. It is possible (on paper) to achieve $\beta^* < 1$ m and also create $\eta^* = \eta^{*'} = 0$ across the C0 IP, as in the Run II design for B0 & D0.

In the efforts presented no attempt is made to re-adjust the tunes to the Run II operating point. C0 gradients are only established at the level that matches into the standard arc optics. Neither is the whole question of separated beams addressed. It became apparent that this whole general approach would have to be abandoned. The reasons for this are summarized in section 3.3.

3.1. $\beta^* = 1.35$ m

Lattice functions & magnets of the standard Collins straight appear below, followed by layout of the C0 straight after being modified for a low-β^* IR.

STANDARD COLLINS C0 STRAIGHT

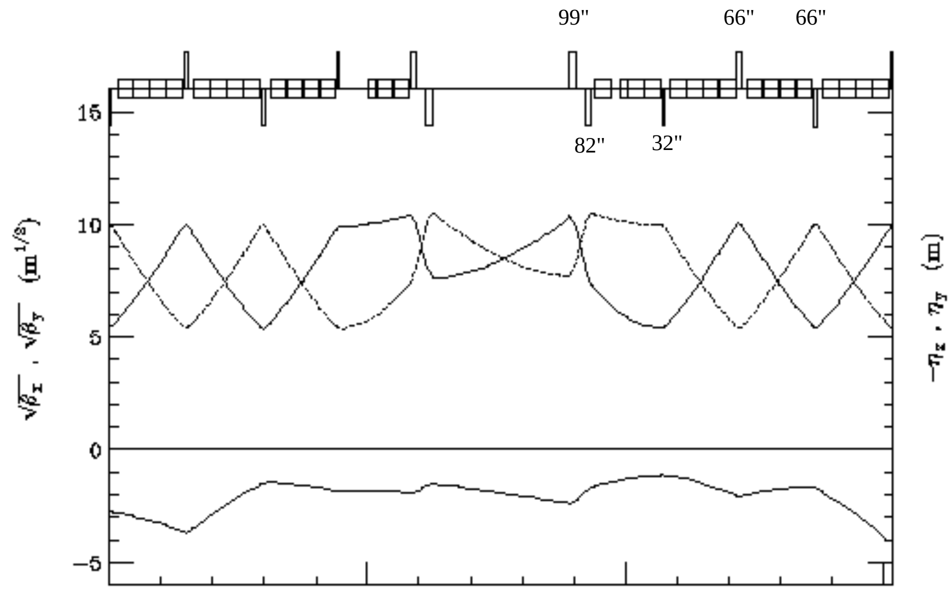

B42 -> C18

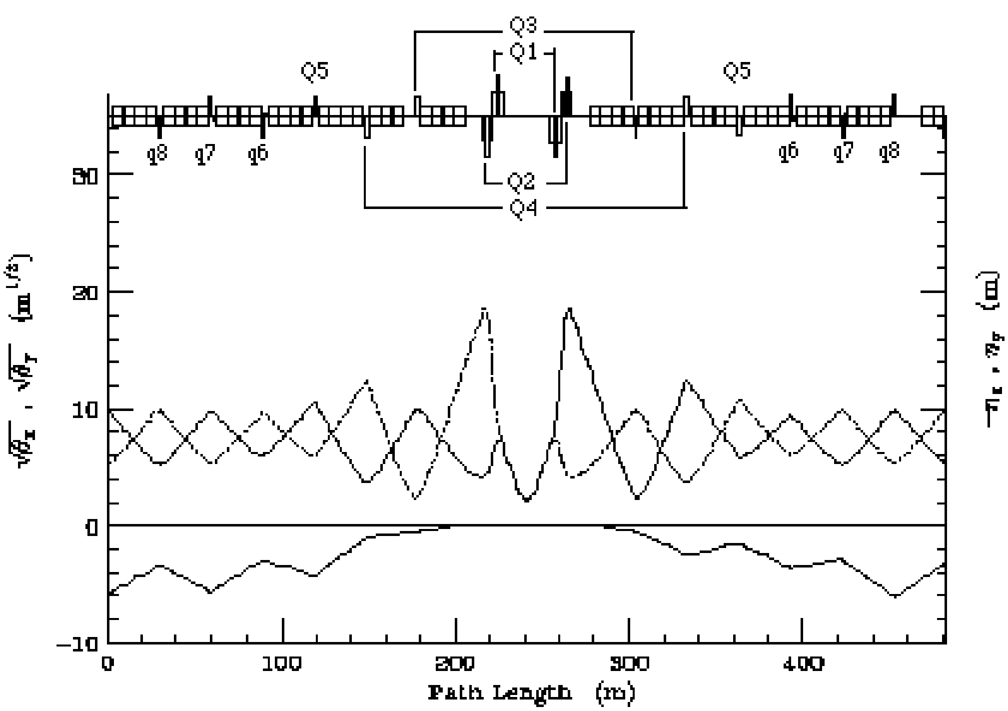

The figure below depicts the approximate layout of the upstream half of the C0 IR straight. The 3 separators & quad conglomerates used to construct the final focus doublets are shown, followed by the full complement of IR quadrupoles and circuits.

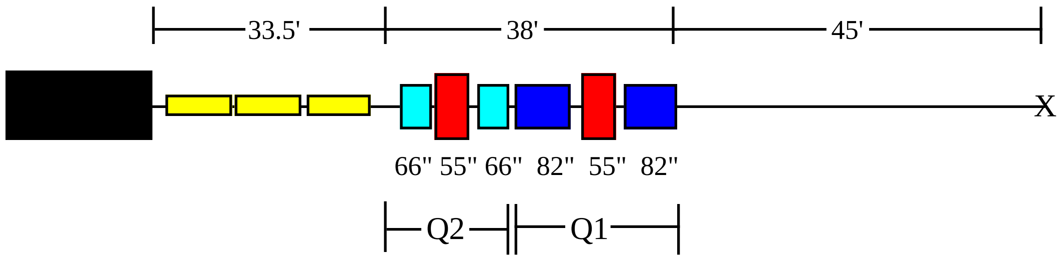

Quad Circuits :

- Q1 : 82" + 55" + 82" quads
- Q2 : 66" + 55" + 66" quads
- Q3 : 90"
- Q4 : 99"
- Q5 : 82"
- q6 : 32"
- q7 : 32"
- q8 : 25"

- The Q1 & Q2 'quads' are composites made from regular gradient 82" & 66" quads (17.155 T/m/kA) plus high gradient 55" quadrupoles (29.018 T/m/kA).

- The Q3 circuit is constructed by replacing the 32" quads at B48-1 & C12-1 with 90" quads.

- Q4 quads are individually powered 99" quads that replace the 66" quads at B47-1 & C13-1.

- The 'trim' quads qt5, qt6, & qt7 are 32", 32", & 25" individually powered Collins quads replacing the regular tune quad spools at those locations.

- The qt8 trims are individually powered regular tune quad spools.

The replacement of the 32" & 66" quads with the much longer 90" & 99" quads has the effect of making the IR insert optically unsymmetric. This is not catastrophic, but it does mean that more quads require independent control than would otherwise be necessary. It also leads to secondary peaks in the arcs that are possibly larger than one would like to see.

Lattice functions & gradients for: (i) injection , and ; (ii) $\beta^* = 1.35$ m appear on the following pages. At all stages of the squeeze $\eta^* = \eta^{*'} \equiv 0$ at the C0 IP.

In the injection lattice it is evident that $\alpha_x = -\alpha_y \neq 0$. There is no real advantage to having $\alpha^* = 0$ for injection, while by allowing it to become non-zero β_{max} can be reduced to $\beta_{max} = 162$ m in the doublet. The maximum integrated gradient limit of 7.00 T·m/m for the qt8 quads prevents further decreases.

At the minimum β^* of 1.35 m the maximum amplitude in the doublet is $\beta_{max} = 1089$ m, which is comparable to the values at B0 & D0 with a β^* of 0.35 m. The limit here is again the maximum field of the qt8 trims, although the Q4 quads are also rapidly approaching their limits at this point.

Maximum gradients encountered during the low-beta squeeze are listed in the following table.

Maximum Gradients from Injection $\beta_{max} = 162$m to $\beta^* = 1.35$m					
Quad	Magnetic Length (in)	Gradient (T/m)	Current (kA)	Gradient (T/m)	Current (kA)
Q1A	82	82.344		82.344	
Q1B	55	139.285	4.800	139.285	4.800
Q1C	82	82.344		82.344	
Q2A	66	82.298		82.298	
Q2B	55	139.207	4.797	139.207	4.797
Q2C	66	82.298		82.298	
Q3	90	74.513	4.344	74.513	4.344
Q4	99	81.600	4.757	78.752	4.591
QT5	32	32.775	1.911	32.906	1.918
QT6 [3]	32	40.665	2.370	37.329	2.176
QT7	25	31.878	1.858	27.059	1.577
QT8 [3]	(30)	9.186	?	9.186	?

[3] Quads QT6 & QT8 reverse polarity during the squeeze.

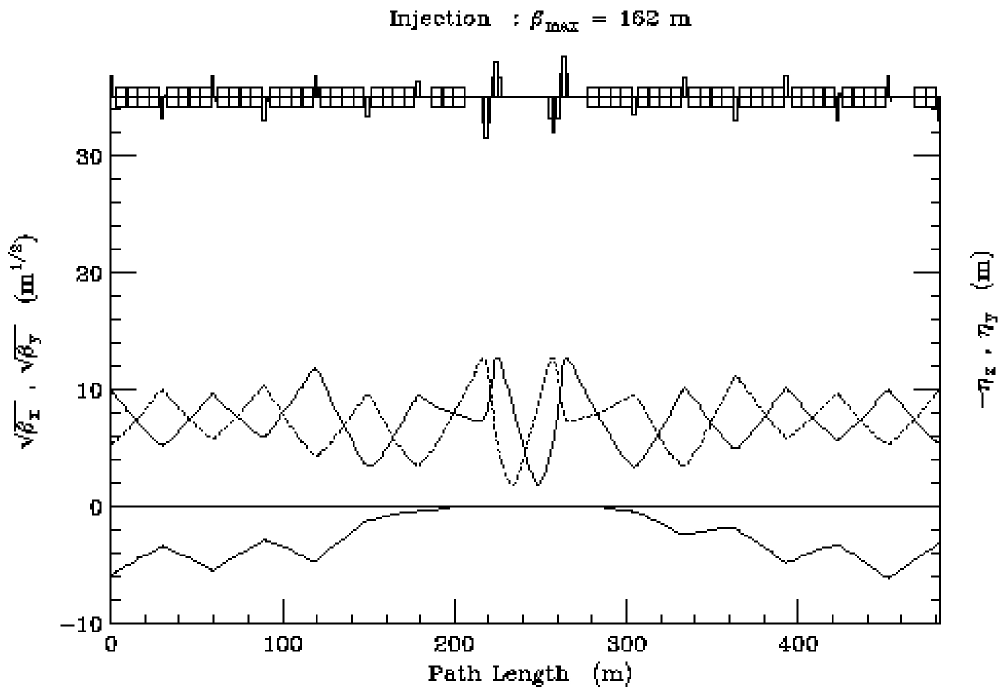

Gradients & Currents at Injection : β_{max} = 162 m

Quad	Magnetic Length (in)	Gradient (T/m)	Current (kA)	Gradient (T/m)	Current (kA)
Q1A	82	70.780		-70.780	
Q1B	55	119.724	4.126	-119.724	4.126
Q1C	82	70.780		-70.780	
Q2A	66	-82.298		82.298	
Q2B	55	-139.207	4.797	139.207	4.797
Q2C	66	-82.298		82.298	
Q3	90	56.277	3.281	-56.277	3.281
Q4	99	-68.694	4.004	66.132	3.855
QT5	32	9.109	0.531	-32.906	1.918
QT6	32	-11.261	0.656	2.444	0.142
QT7	25	-15.728	0.917	14.503	0.845
QT8	(30)	9.186	?	-9.109	?

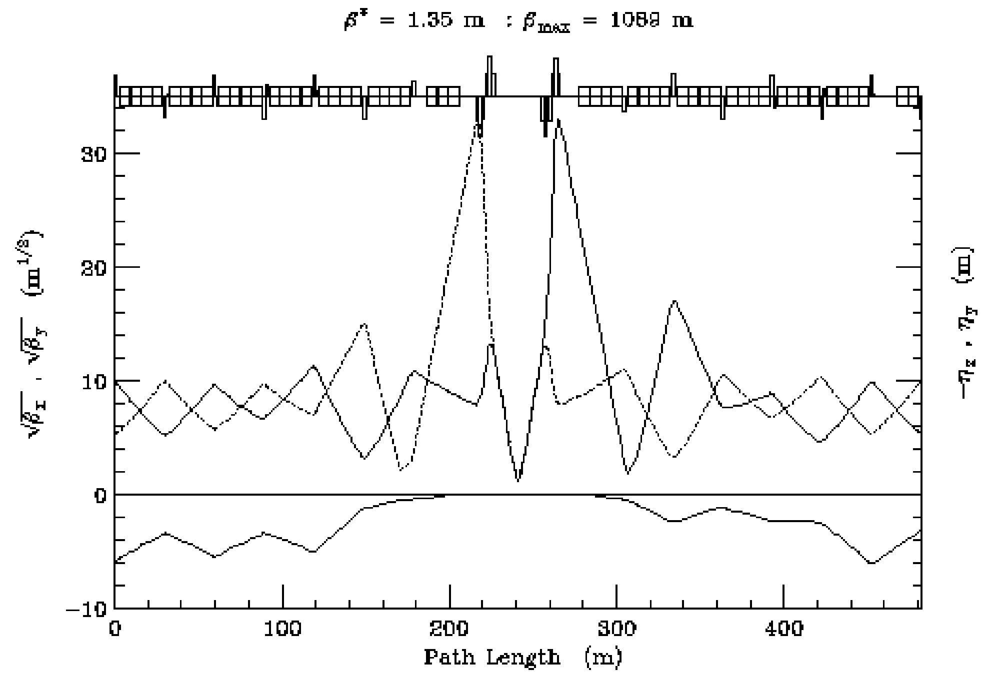

Gradients & Currents at $\beta^* = 1.35$ m					
Quad	Magnetic Length (in)	Gradient (T/m)	Current (kA)	Gradient (T/m)	Current (kA)
Q1A	82	82.089		-82.089	
Q1B	55	138.854	4.785	-138.854	4.785
Q1C	82	82.089		-82.089	
Q2A	66	-81.547		81.547	
Q2B	55	-137.936	4.754	137.936	4.754
Q2C	66	-81.547		81.547	
Q3	90	56.040	3.267	-56.040	3.267
Q4	99	-81.285	4.738	79.345	4.625
QT5	32	23.147	1.349	-23.371	1.362
QT6	32	40.665	2.370	-37.329	2.176
QT7	25	-31.878	1.858	27.059	1.577
QT8	(30)	8.231	?	9.186	?

3.2. $\beta^* \leq$ 1.00 m

Lower values of β^* than the 1.35 m achieved in the preceding section can be reached either by extending the previous design farther into the arcs with qt9 (or beyond) trim quads or by powering more main arc magnets independently. One example of lattice functions & quad circuits obtained with the latter approach is illustrated below.

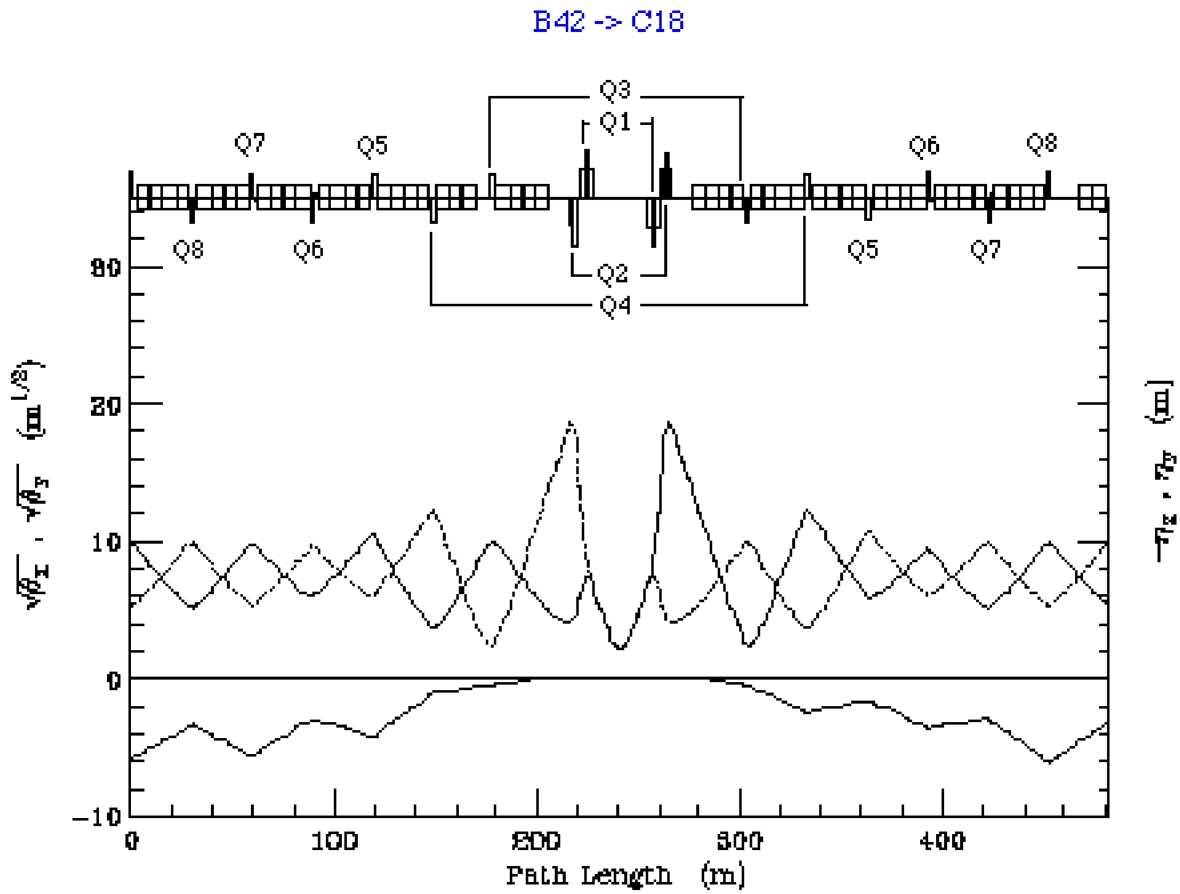

Quad Circuits :

- Q1 : 99" + 55" + 66" quads
- Q2 : 66" + 55" + 66" quads
- Q3 : 90"
- Q4 : 99"
- Q5 : 82"
- Q6 : 66"
- Q7 : 66"
- Q8 : 66"

This model is very similar to that of the preceding design from B47 $\rightarrow$ C13, with only minor changes made to the Q1 quad composition. The big design differences occur from B43 $\rightarrow$ B46 & from C14 $\rightarrow$ C17. Rather than using 25" & 32" 'trim' quads at these locations, the main arc magnets here are also powered independently.

- The Q1 & Q2 'quads' are composites made from regular gradient 99" & 66" quadrupoles (17.155 T/m/kA) plus high gradient 55" quads (29.018 T/m/kA).

- The Q3 circuit is constructed by replacing the 32" quads at B48-1 & C12-1 with 90" quads.

- Q4 quads are individually powered 99" quads that replace the 66" quads at B47-1 & C13-1.

- Q5's are individually powered 82" quads replacing the 66" quads at B46-1 & C14-1.

- Q6, Q7, & Q8 quads are individually powered standard 66" arc quads.

The magnets in this design are capable of creating a beta as small as $\beta^* = 0.60$ m, while maintaining $\eta^*=\eta^{*\prime}= 0$ across the IP. As the following graph demonstrates, however, this results in a maximum β in the doublet of about $2^1/_2$ kilometers, which is clearly not a solution the Tevatron can support. A β^* of ~1 m is about the smallest value compatible with keeping β_{max} comparable to the values at CDF & D0.

Subsequent pages present the lattice functions & gradients for $\beta^* = 1$ m and for the injection lattice, plus graphs quad current variations during the squeeze.

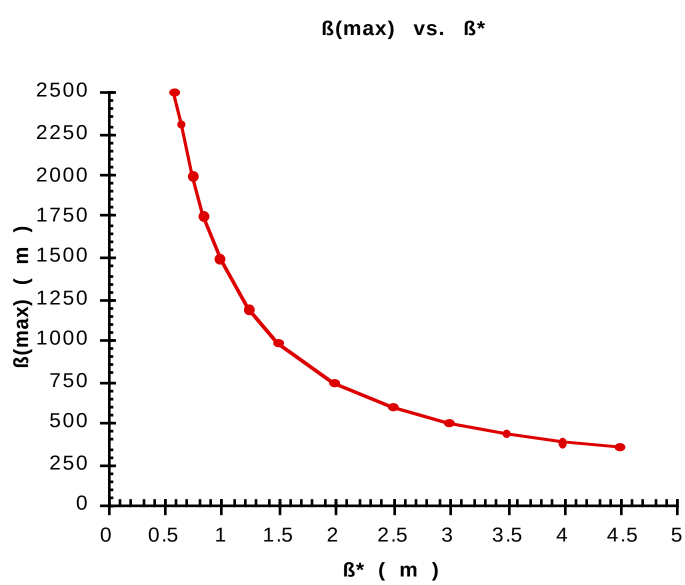

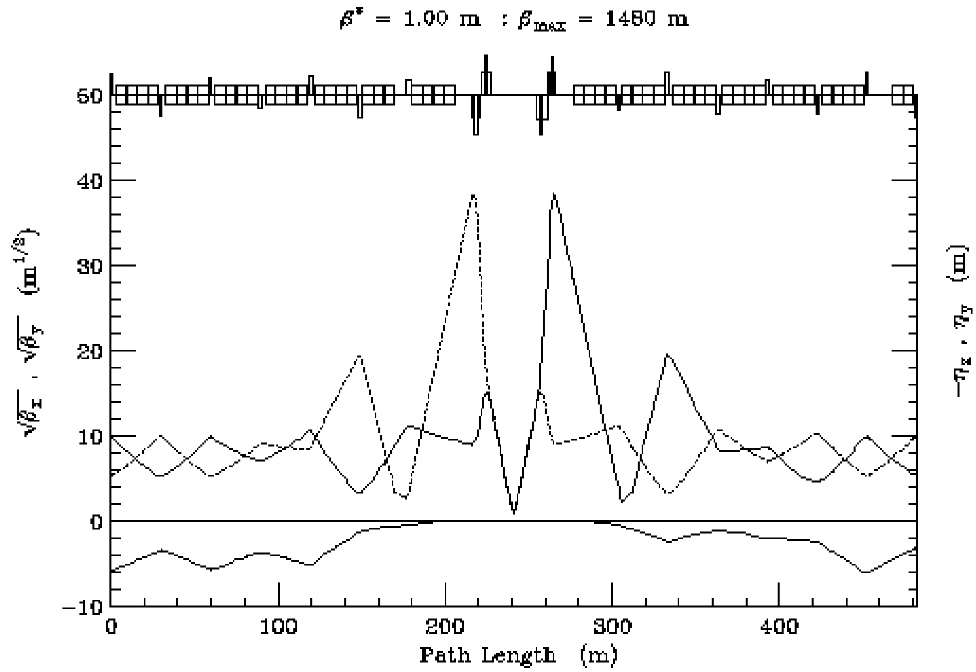

Gradients & Currents at β^* = 1.00 m					
Quad	Magnetic Length (in)	Gradient (T/m)	Current (kA)	Gradient (T/m)	Current (kA)
Q1A	66	82.605		-82.605	
Q1B	55	139.726	4.815	-139.726	4.815
Q1C	99	82.605		-82.605	
Q2A	66	-81.717		81.717	
Q2B	55	-138.224	4.763	138.224	4.763
Q2C	66	-81.717		81.717	
Q3	90	51.958	3.029	-51.958	3.029
Q4	99	-80.431	4.689	80.431	4.689
Q5	82	66.769	3.892	-66.978	3.904
Q6	66	-45.732	2.666	52.320	3.050
Q7	66	62.905	3.667	-64.560	3.763
Q8	66	-75.831	4.420	81.300	4.739

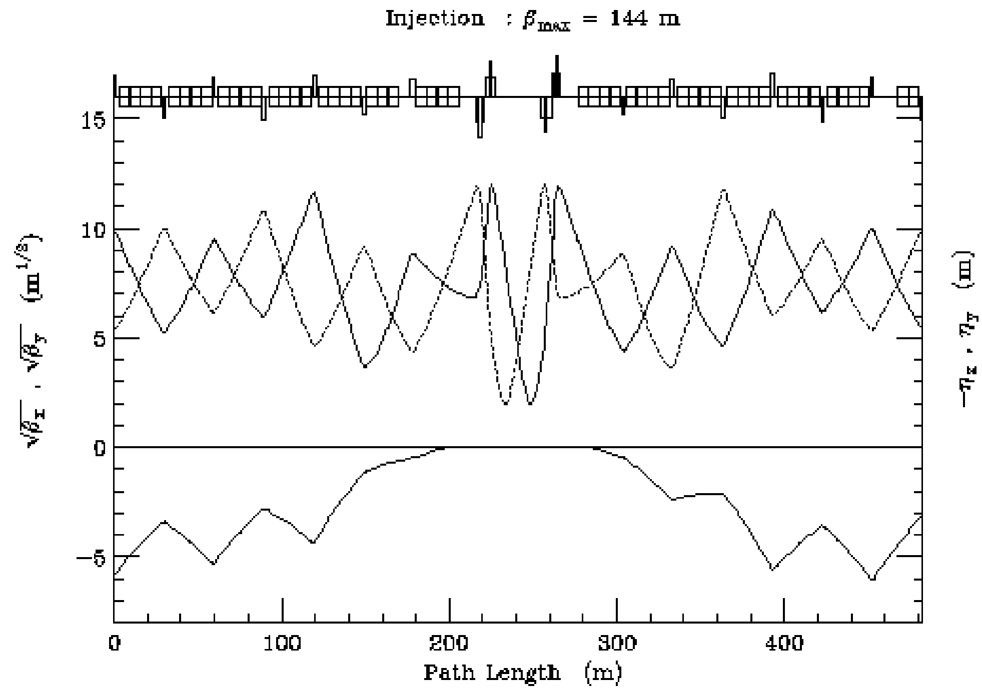

Gradients & Currents at Injection : β_{max} = 144 m					
Quad	Magnetic Length (in)	Gradient (T/m)	Current (kA)	Gradient (T/m)	Current (kA)
Q1A	66	69.878		-69.878	
Q1B	55	118.198	4.073	-118.198	4.073
Q1C	99	69.878		-69.878	
Q2A	66	-79.656		79.656	
Q2B	55	-134.738	4.643	134.738	4.643
Q2C	66	-79.656		79.656	
Q3	90	57.607	3.358	-57.607	3.358
Q4	99	-60.622	3.538	60.622	3.538
Q5	82	71.735	4.182	-71.501	4.168
Q6	66	-78.519	4.577	78.903	4.599
Q7	66	70.056	4.084	-68.705	4.005
Q8	66	-69.579	4.056	68.666	4.003

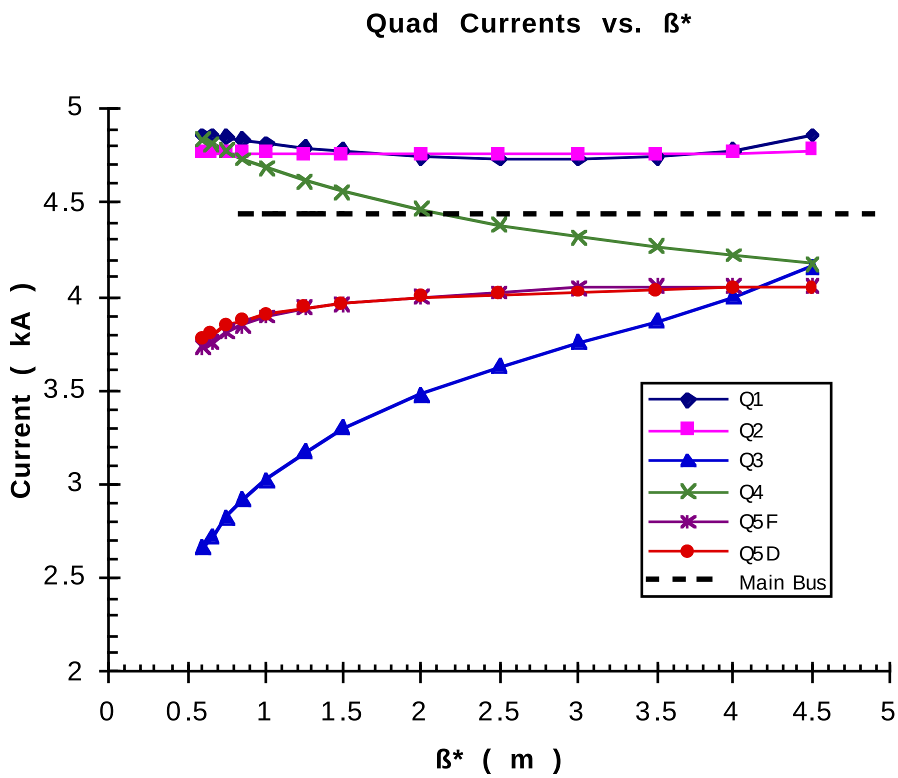

Quad Currents vs. ß*
Current (kA)
ß* (m)
Q1
Q2
Q3
Q4
Q5F
Q5D
Main Bus

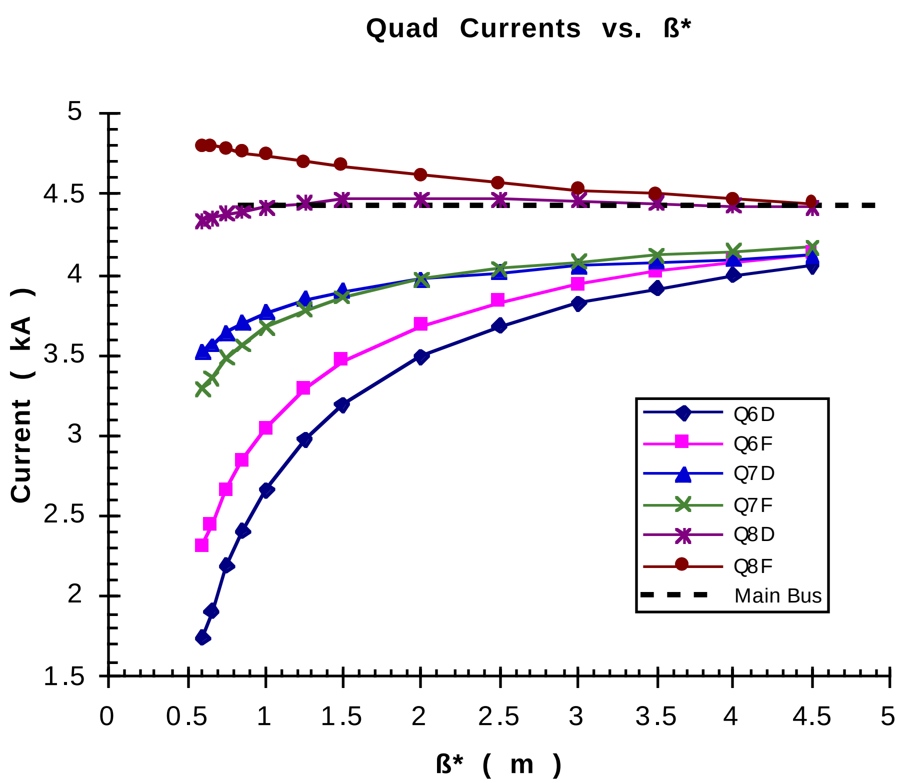

Quad Currents vs. ß*
Current (kA)
ß* (m)
Q6D
Q6F
Q7D
Q7F
Q8D
Q8F
Main Bus

3.3. Design Defects & Fatal Flaws

Both of the models described so far assumed space for 3 separators each side of the IP, the same as there are at B0 & D0. However, with a doublet final focus rather than a triplet, 3 is not the optimum number. Across the separators at the 3 Tevatron IR's the ratios of β functions are approximately:

$$\text{B0 \& D0} \qquad \sqrt{\beta_{x,y}/\beta_{y,x}} \approx 2 \qquad ;$$

$$\text{C0} \qquad \sqrt{\beta_{x,y}/\beta_{y,x}} \approx 3 \qquad .$$

So, at B0 & D0, effectively equal kicks in the two planes are achieved by having 2 separators in the plane with the smaller β and 1 separator in the other plane. At C0 though, β in one plane is roughly 9x that of the other. The optimum number of separators is therefore 4, with 3 in the plane of smaller β. As will be discussed later, it is not possible to generate sufficient space to accommodate 4 separators.

A severe problem with this approach to insert design is that magnets can probably only be powered independently in the arcs at the expense of losing the spool packages and, therefore, the valuable correction elements they contain. The layout of a typical arc quadrupole site is sketched below.

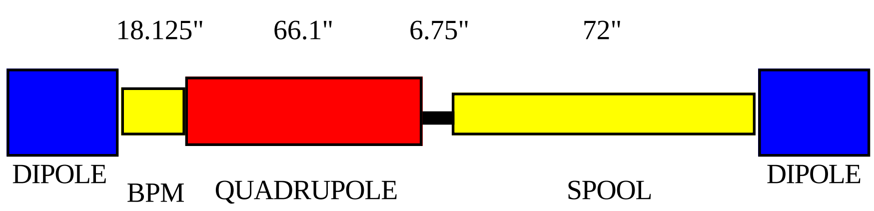

In the model described in section 3.1, spools at the B44 → B46 & C14 → C16 locations were replaced with 25" & 32" Collins quads. The standard length of a Tevatron power feed is 29" and the necessary cold by-passes consume ~29" more space. This definitely eliminates the spool piece and -- doing the arithmetic & consulting the drawing above -- it is clear that the feed & by-passes would need to be re-designed if the BPM is to be saved.

The second design (section 3.2) is similarly flawed. In that model the arc quads are powered independently at the B44 → B46 & C14 → C16 sites. Again, the power feed & cold by-pass will eat up 58", which again eliminates the spool package. One small consolation is that, in this case, at least the feed & by-passes don't have to be re-engineered as well to avoid sacrificing the BPM.

Supposing that some acceptable solution could be found for these problems in the arc, the death knell for this approach sounds, nonetheless, once the doublet is studied more closely. To obtain <u>any</u> β^*a (lower) estimate for the quadrupole lengths required can be obtained by assuming that particles parallel to the beam axis entering the doublet are focused into the IP.

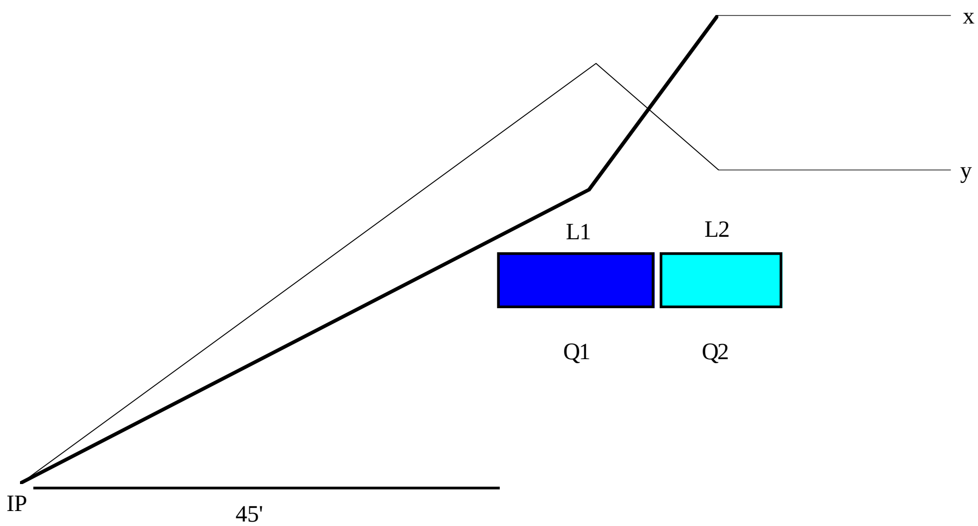

With quad gradients of 85.775 T/m (regular quads @ 5.000 kA), it can be demonstrated that parallel-to-point focusing using a doublet at C0 requires at least 38' of magnets (this does not take into account any connections between them - that's additional). From the IP to the first arc dipole is 116'6". The detector eats up 45', and the doublet another 38'. This leaves only 33'6" for everything else.

The following is a minimal list of additional hardware that must appear for operation:

1 S-Spool	: 6'
1 Power Feed	: 3'
2 BPMs	: 2'
1 TAB	: 2'
Total	:13'

Only 20'6" of 'free' space remains for separators! Spaces occupied by various separator bits are:

1 Separator module	: 10' 6$^1/_2$"
2 Separator modules	: 19' 7$^1/_8$"
3 Separator modules	: 28' 7$^3/_4$"
Cold By-pass	: 2' 5"
Power Feed	: 2' 5"

So:

1 Separator plus ancillary hardware	: 15' 4$^1/_2$"
2 Separators plus ancillary hardware	: 24' 5$^1/_8$"
3 Separators plus ancillary hardware	: 33' 5$^3/_4$"

The conclusion is that there is really only room for one separator, which is clearly unacceptable.

3.4. Summary

The powering of individual arc quads leads to the loss of all the correction elements residing in the spool packages. Even if this problem could be surmounted, it does not appear that an adequate number of separators can co-exist with a doublet final focus created solely from existing magnets. This points towards two equally senseless solutions: (i) either a low-beta can be formed, but without colliding beams, or; (ii) the beams can be made to collide, but not at low beta.

4. QUARTER-WAVE TRANSFORMER

The principle of the $\lambda/4$-transformer matching technique is illustrated in the accompanying picture. Q4 quadrupoles are located a quarter of a Tevatron cell away from the B47 & C13 quads. In the middle of a regular Tevatron half-cell $\beta_x=\beta_y \approx 53.3$ m and $\alpha_x= -\alpha_y \approx \pm 1.22$. The Q1, Q2, & Q3 circuits form a doublet/triplet hybrid that takes $\beta_x = \beta_y = \beta^*$, $\alpha_x = \alpha_y = 0$ [4] at the IP and matches to $\beta_x = \beta_y \approx 53$ m and $\alpha_x = -\alpha_y = \alpha_{mid}$ at the Q4 locations. Gradient adjustments to Q4 do not affect β (in thin lens approximation) but change α_x & α_y equally by amounts $\Delta\alpha_{mid} \approx \pm\alpha_{mid}/f_4$, where f_4 is the focal length of the Q4 quadrupole. Tuning with Q4 to obtain $\alpha_x = -\alpha_y \approx \pm 1.22$ then completes the α, β match into the regular Tevatron arcs. Trim quads at B43, B44, B46, B47, and C13, C14, C16, C18 are powered independently for extra fine α, β matching.

[4] $\alpha^* \equiv 0$ is the optimum choice for creating beam separation away from the IP by creating 90^o of phase between the IP and separators on both sides.

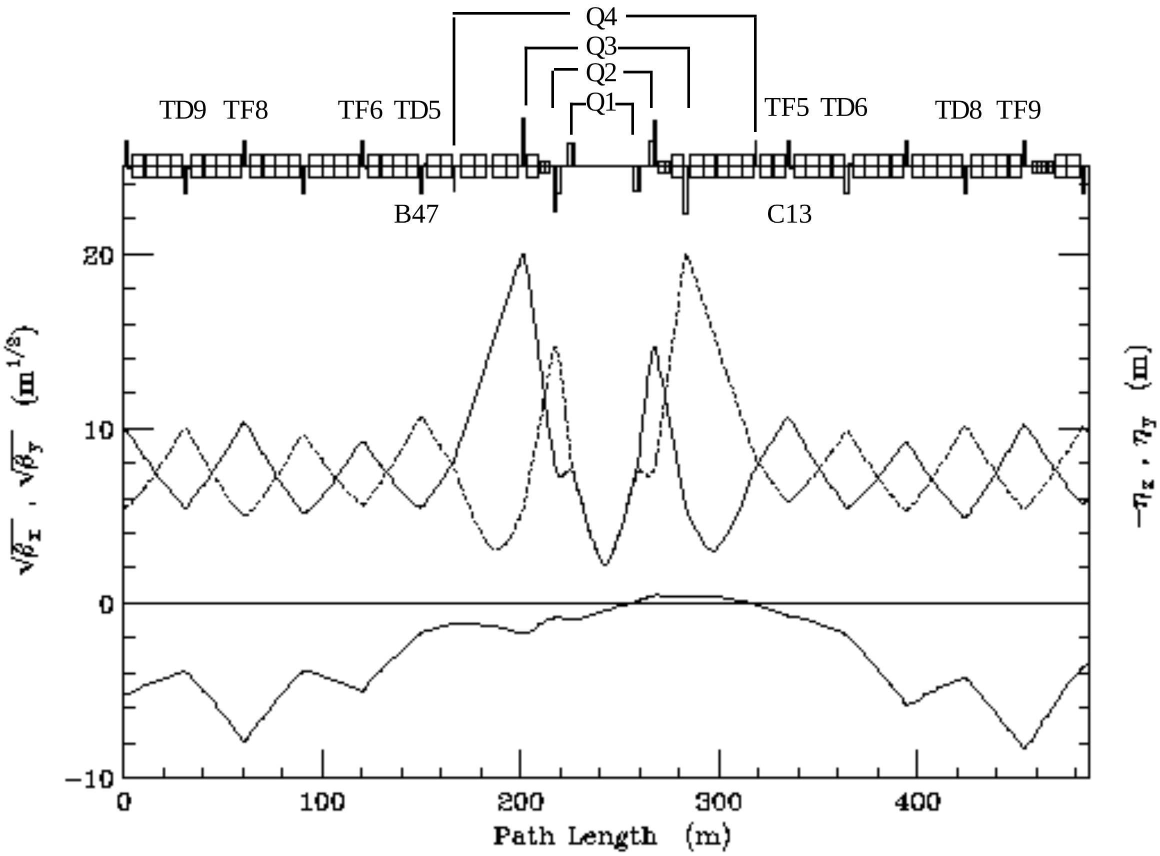

An attractive feature of this particular approach is that by matching α, β directly into the middle of a regular Tevatron cell no secondary peaks are formed, as might otherwise occur when fitting from a non-FODO to FODO lattice. This technique has been applied successfully in the arc-to-high–β transition match in the Recycler, and in studies for a high dispersion - low–β Recycler insert. This simple trick alone, though, does nothing to address dispersion matching – that problem is largely left to the trim quads. The maximum gradients these 8 trim quads are allowed to assume represents the only physical difference between the IR designs presented in sections 4.1 & 4.2.

The doublet Q1 & Q2 'quadrupoles' are constructed from 2 magnets each. Two separators are installed between the Q2 quads and 1st dipole at the B49 & C11 locations. After considerable experimentation, the site of the Q3 quads was chosen to minimize gradients in the Q1, Q2, & Q3 magnets, minimize β_{max}, and to produce $\sqrt{\beta_x} \approx \sqrt{\beta_y}$ at the midpoints of the horizontal and vertical separators. The Q4 magnets are located a quarter-cell away from the B47 & C13 quadrupoles. .

In the IR designs of both section 4.1 & section 4.2 the major quad circuits are composed of the following magnets:

Q1	A	:	66"	(17.155 T/m/kA)
	B	:	66"	(17.155 T/m/kA)
Q2	A	:	99"	(17.155 T/m/kA)
	B	:	55"	(29.018 T/m/kA)
Q3		:	55"	(29.018 T/m/kA)
Q4		:	32"	(17.155 T/m/kA)

The 7 dipoles between the Q2 quadrupole & B47 on the upstream end, and the 8 dipoles between Q2 & C13 downstream, are moved to make space for the Q3 & Q4 magnets. Upstream dipole positions are adjusted to re-close the orbit, while retaining sufficient space for the synch light monitor.

4.1. 37.0 T·m/m Trim Quads

In this preliminary (optimistic) exploration of an IR design using the quarter-wave matching technique the strengths of the 8 trim quads are unconstrained. It is possible to then reach $\beta^* < 5$m at C0, and also to create $\eta^*=\eta'^*=0$ dispersion-free IR's at all 3 interaction points in the Tevatron.

4.1.1. Tune Re-adjustment

Addition of a low β at C0 raises the machine tunes by a half-integer from their Run II values of ~20.5, right onto the integer resonance at 21.0. The ideal way to re-adjust the tunes is to leave the long B0 $\rightarrow$ D0 arc phases unchanged from their Run II values, while adding or subtracting roughly a half-integer through the short B0 $\rightarrow$ C0 $\rightarrow$ D0 section. Leaving the long arc undisturbed has obvious attractions -- separators, collimators, correction schemes, whatever, would continue to function just as before. Changing the short section by 1/2 is also beneficial -- making head-on collisions at C0 possible when all 3 IPs are at collision. This otherwise does not appear possible, and a C0 crossing angle becomes unavoidable. The second choice for tune re-adjustment is to change the long arc tune by 1/2. This ensures that at least the separators can still be made to work. The drawback to both these approaches is that, with the B & C sector tune strings powered differently than the D, E, F, & A quads, for any β^* the IR gradients are different at B0 & D0.

Attempts to implement both of these options to re-adjust the tunes were made. Neither worked. The tune quad strings have insufficient strength to change the tunes by ±1/2 while simultaneously maintaining an optical match to the B0 & D0 IP's. Furthermore, even with tune re-adjustment distributed over all 6 sextants, it is still not possible to re-establish the Run I & II tunes. A new operating point was therefore established, with the model tunes set between the 4/5 & 5/6 resonances, at (20.8167, 20.8167) [5,6]. This is the same fractional tune as RHIC.

The addition of a 3rd IR results in the phase advance from place-to-place in the ring becoming completely different from the Run II design. This has profound implications for machine operations. In essence, the Tevatron becomes a completely new machine.

At the new operating point, the following pages outline the lattice functions & quadrupole gradients for 2 operating scenarios:

(i) all 3 IP's at collision (β^*= 0.35m @ B0 & D0, and β^*= 5.00m at C0)

(ii) injection (β^*= 1.60m @ B0 & D0, and β^*= 8.00m at C0)

ALL 3 IP's at COLLISION :

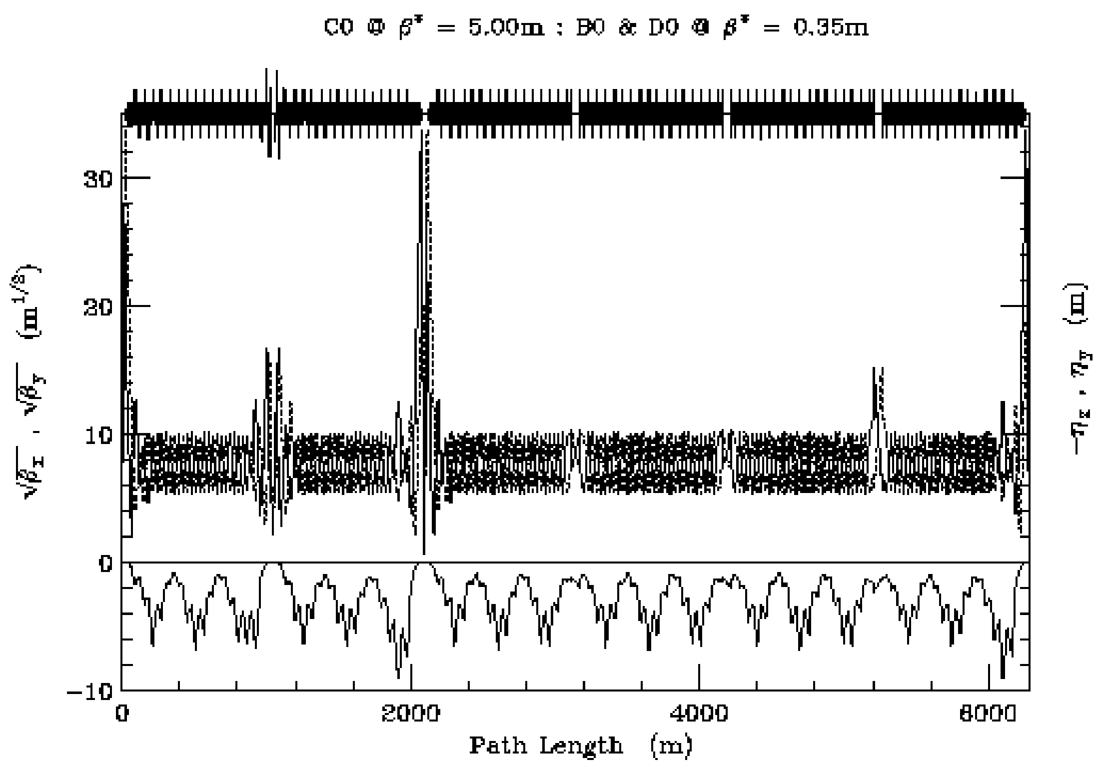

---

[5] Appendix II : Tune Space from 20.5 → 20.9.
[6] Appendix III : The Bed of Nails.

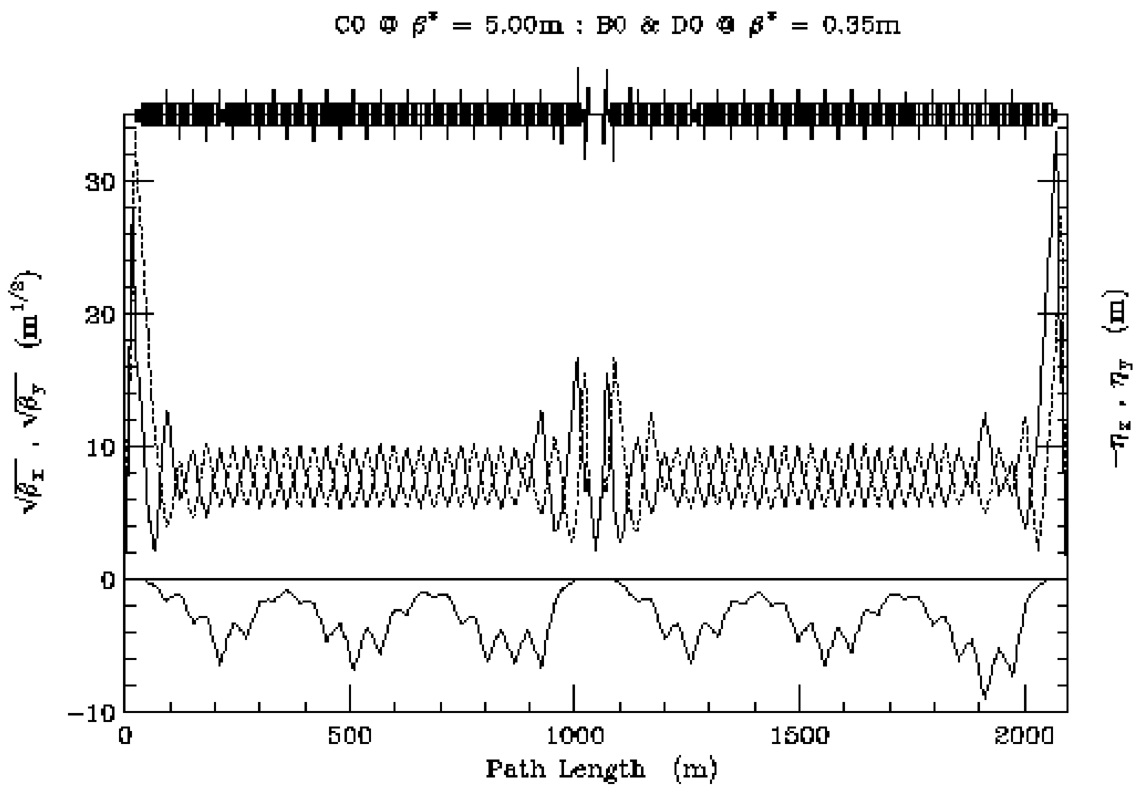

Quad #	β* = 5.00 m up	down
Q1	4.783 kA	-4.783 kA
Q2	-4.676 kA	4.676 kA
Q3	4.916 kA	-4.916 kA
Q4	-4.719 kA	4.719 kA
T5	-0.5637 T/m	-2.2451 T/m
T6	**-24.366 T/m**	**24.652 T/m**
T8	**23.685 T/m**	**-27.227 T/m**
T9	-8.9879 T/m	8.1733 T/m

INJECTION :

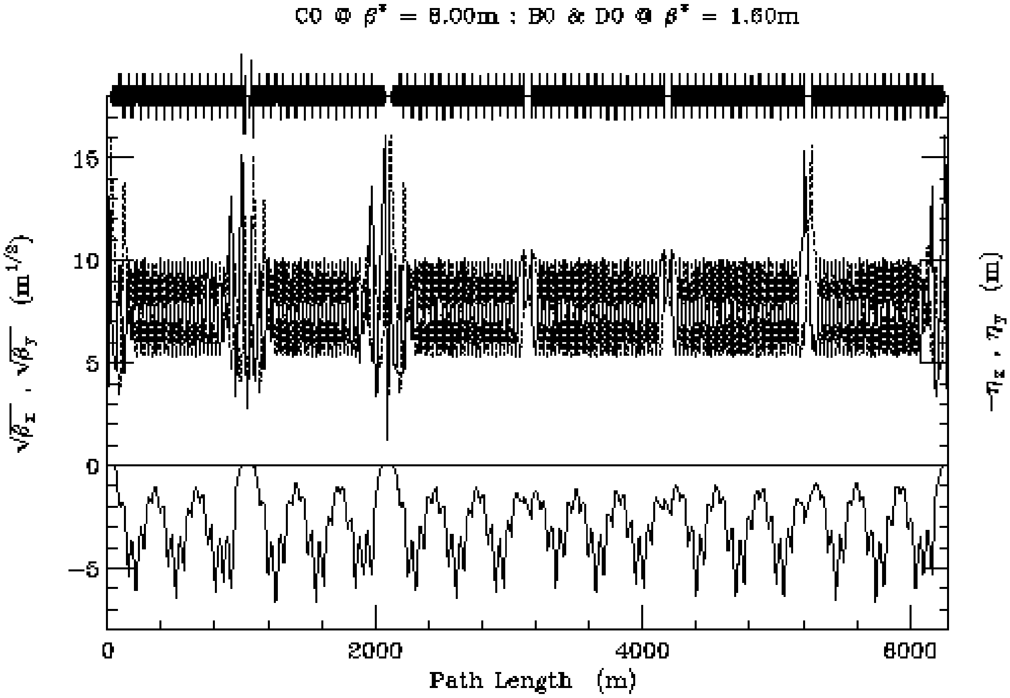

C0 @ β^* = 8.00m : B0 & D0 @ β^* = 1.60m
15
10
5
0
−5
0
2000
4000
6000
Path Length (m)
$\sqrt{\beta_x}$, $\sqrt{\beta_y}$ ($m^{1/2}$)
$-\eta_x$, η_y (m)

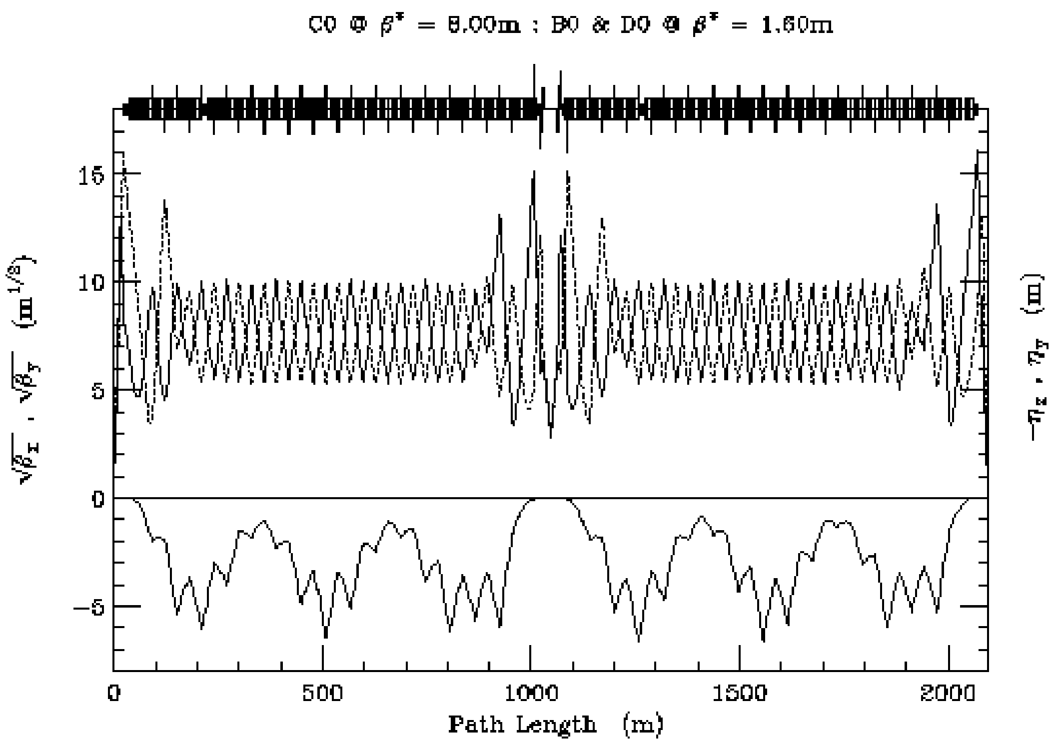

C0 @ β^* = 8.00m : B0 & D0 @ β^* = 1.60m
15
10
5
0
−5
0
500
1000
1500
2000
Path Length (m)
$\sqrt{\beta_x}$, $\sqrt{\beta_y}$ ($m^{1/2}$)
$-\eta_x$, η_y (m)

Quad #	β^* = 8.00 m	
	up	down
Q1	4.213 kA	-4.213 kA
Q2	-4.365 kA	4.365 kA
Q3	4.876 kA	-4.876 kA
Q4	-1.182 kA	1.182 kA
T5	**13.588 T/m**	**-15.127 T/m**
T6	**-30.431 T/m**	**29.248 T/m**
T8	**27.613 T/m**	**-30.521 T/m**
T9	**-16.495 T/m**	**12.887 T/m**

This preliminary lattice design shows some promise of being able to fulfill most of the optical restrictions listed in Section 2. The injection & collision lattices display similar characteristics:

- β-wave < ±3 % in the arcs.
- Dispersion < 7 m in the arcs.
- At B0 & D0 $\eta^* = \eta'^* = 0$.
- $\eta^* = \eta'^* = 0$ at C0 was obtained as a bonus.

A solution for a β^* of 5 m was presented, but with fairly straightforward magnet substitutions at the Q4 locations it appears that a $\beta^* \leq 2$ m might be reached. Complete solutions for all the desired operating scenarios listed in Section 2 have not been attempted, but no serious obstacles are readily apparent.

Unfortunately, this design must be rejected. This C0 insert can not be built solely from existing magnet spares. The trim quad gradients highlighted in the tables are much higher than can be physically realized by the existing spool quads. These strengths could only be attained by building new spool pieces -- probably of the Bartelson type installed at B0 & D0 IR's.

4.2. 7.0 T·m/m Trim Quads

The latest (& final) incarnation of the C0 IR design is essentially identical in layout to the one described in section 4.1; the major exception being that the high gradient Bartelson-like spools in the model are replaced with regular tune quad spools [7]. The single, most significant result of switching to these much weaker trim quads is that dispersion can neither be controlled across the C0 IR nor matched to the regular arc dispersion. The large dispersion wave thus generated has a significant impact on the matching abilities at the B0 & D0 IR's as well.

With the new tunes of (20.8167, 20.8167), four possible operating scenarios have been studied:

(i) all 3 IP's at collision	(β^*= 0.35m @ B0 & D0, and β^*= 5.00m at C0)
(ii) injection	(β^*= 1.75m @ B0 & D0, and β^*= 10.00m at C0)
(iii) B0 & D0 at collision : not C0	(β^*= 0.35m @ B0 & D0, and β^*= 10.00m at C0)
(iv) C0 at collision : not B0 & D0	(β^*= 1.75m @ B0 & D0, and β^*= 5.00m at C0)

Although optical solutions for these various operating modes exist, these solutions do not satisfactorily meet any of the optics restrictions (1)-(11) listed in Section 2. Lattice functions & the corresponding gradients for these 4 scenarios appear on subsequent pages.

[7] see Appendix IV for the complete layout of the C0 IR from B47 → C13.

Collision Optics for 3 IP's

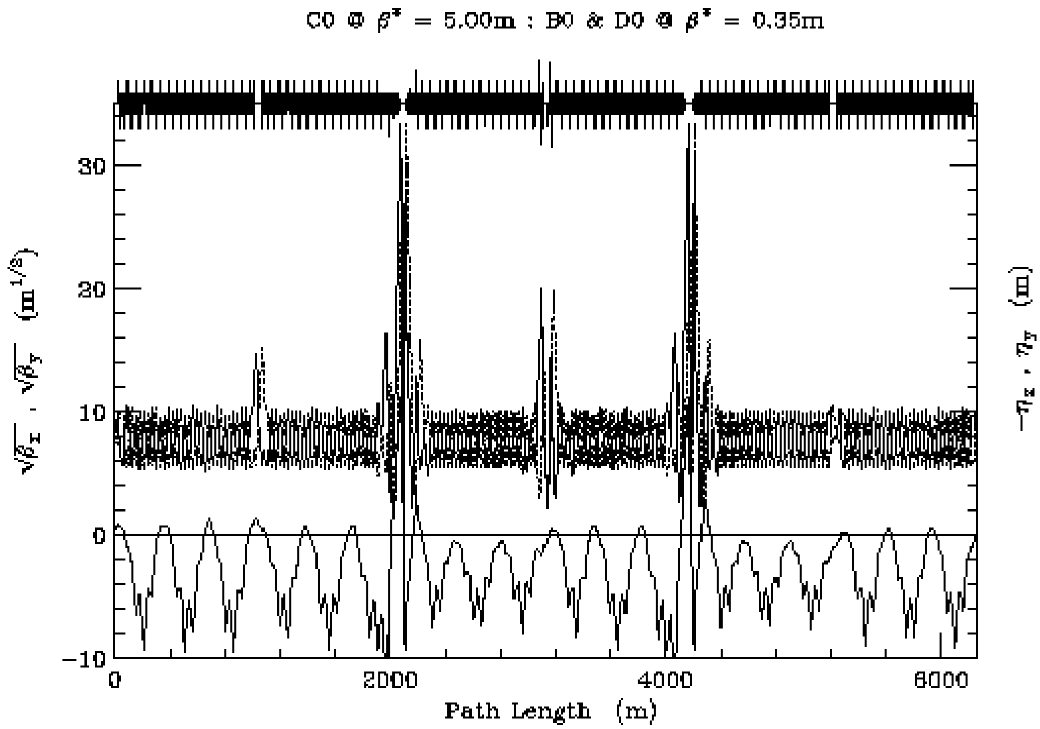

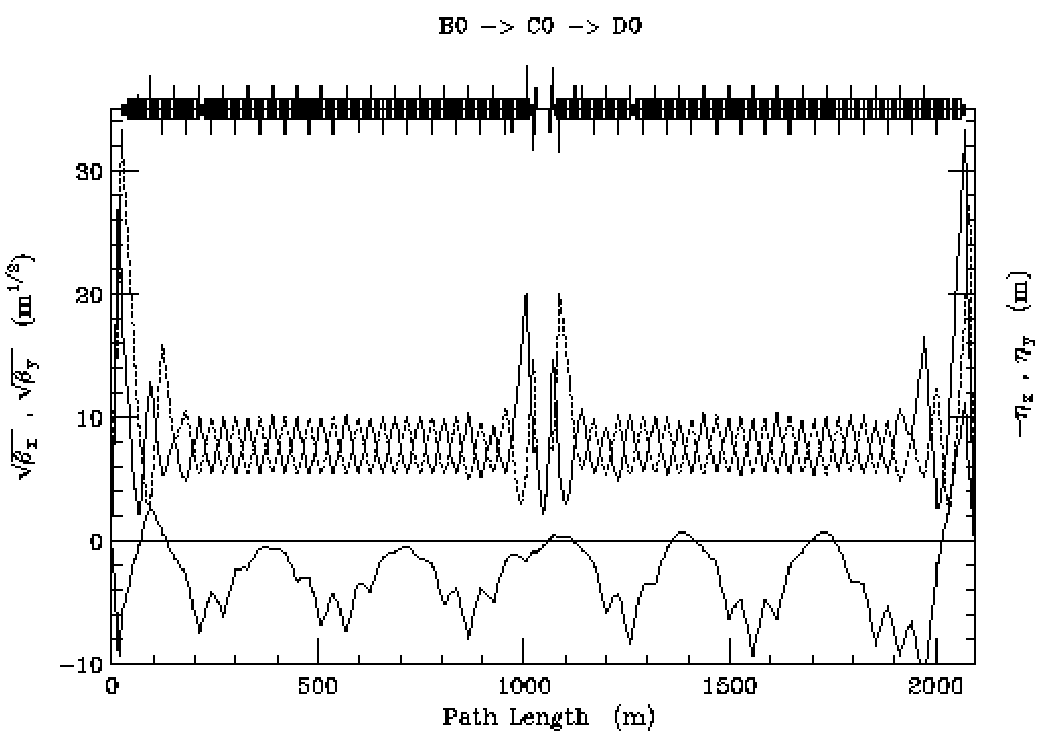

1 TeV Gradients for Collisions @ B0, C0, & D0

Quad #	C0 @ β^* = 5.00 m up	C0 @ β^* = 5.00 m down
Q1	4.128 kA	-4.128 kA
Q2	-4.508 kA	4.508 kA
Q3	4.715 kA	-4.715 kA
Q4	-4.232 kA	4.232 kA
TQ5	6.847 T/m	-6.051 T/m
TQ6	-4.220 T/m	**8.573 T/m**
TQ7	0	0
TQ8	4.085 T/m	-0.879 T/m
TQ9	-4.821 T/m	2.980 T/m

Quad #	B0 & D0 @ β^* = 0.35 m up (T/m)	B0 & D0 @ β^* = 0.35 m down (T/m)
Q4	139.971	-139.971
Q3	-138.117	138.117
Q2	139.971	-139.971
Q1		
Q5	-47.181	47.181
Q6	-107.324	107.324
T6	-3.854	
T7	45.325	-47.765
T8	**-8.754**	2.712
T9	-52.702	54.100
T0	-8.782	5.051
TB	**-8.498**	

QFA4 = –6.5161 T/m : (μ_x, μ_y) = (20.8167, 20.8167)

QDD1 = 4.6756 T/m :

- 9.186 T/m maximum for : TQ5, TQ6, TQ8, TQ9, & T6, T8, TB
- 58.268 T/m maximum for : T7, T9, T0

Injection Optics

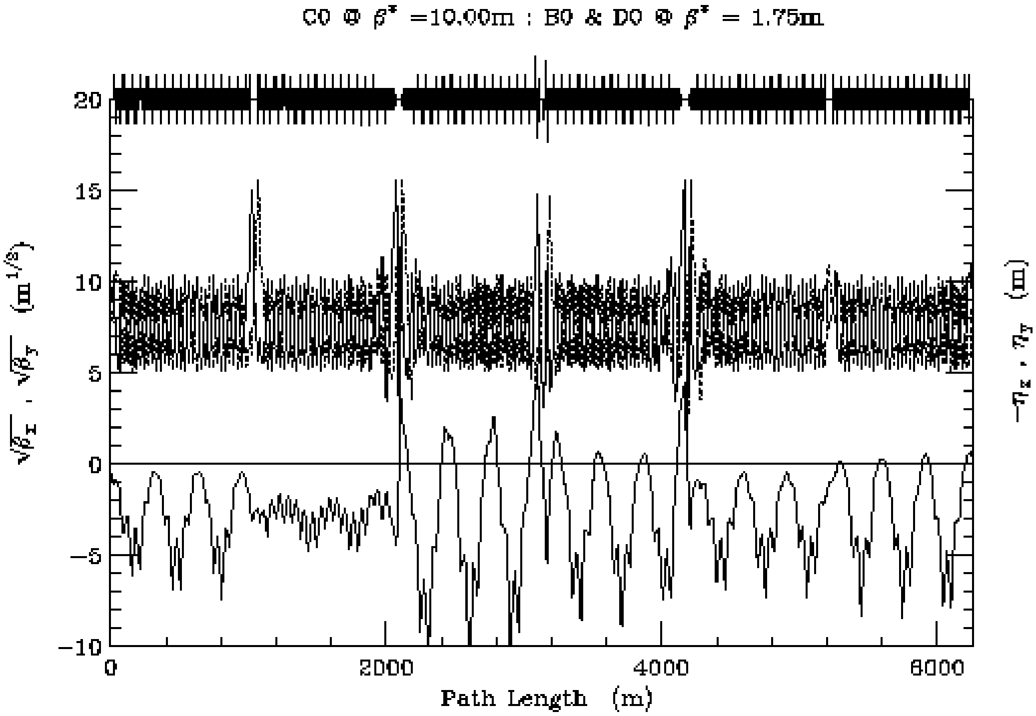

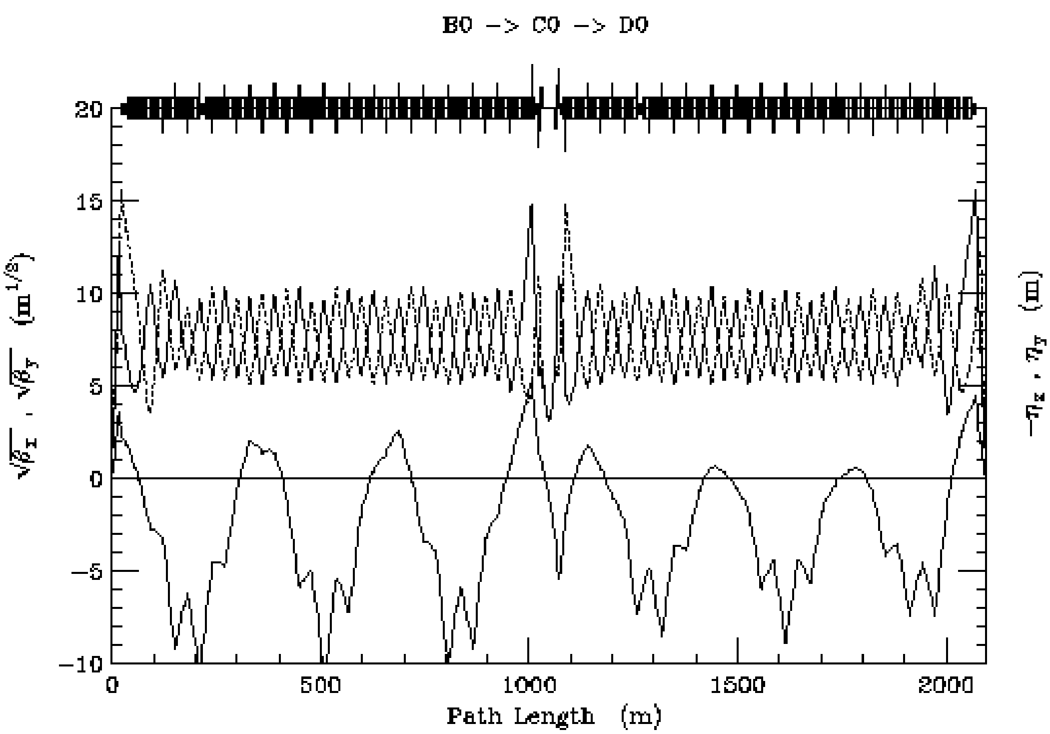

1 TeV Gradients for Injection

Quad #	C0 @ β^* = 10.00 m up	down
Q1	3.718 kA	-3.718 kA
Q2	-4.189 kA	4.189 kA
Q3	4.613 kA	-4.613 kA
Q4	-1.895 kA	1.895 kA
TQ5	7.531 T/m	-5.558 T/m
TQ6	**8.819 T/m**	-5.719 T/m
TQ7	0	0
TQ8	-0.917 T/m	3.224 T/m
TQ9	-3.856 T/m	-2.399 T/m

Quad #	B0 & D0 @ β^* = 1.75 m up (T/m)	down (T/m)
Q4	132.112	-132.112
Q3	-133.641	133.641
Q2	132.112	-132.112
Q1		
Q5	32.374	-32.374
Q6	-11.154	11.154
T6	-1.022	
T7	38.687	-40.981
T8	**8.778**	-6.865
T9	-14.744	19.837
T0	15.586	-18.923
TB	8.562	

QFA4 = –0.8316 T/m : (μ_x, μ_y) = (20.8167, 20.8167)
QDD1 = –1.5313 T/m :

- 9.186 T/m maximum for : TQ5, TQ6, TQ8, TQ9, & T6, T8, TB
- 58.268 T/m maximum for : T7, T9, T0

Optics for B0 & D0 @ Collision : Not C0

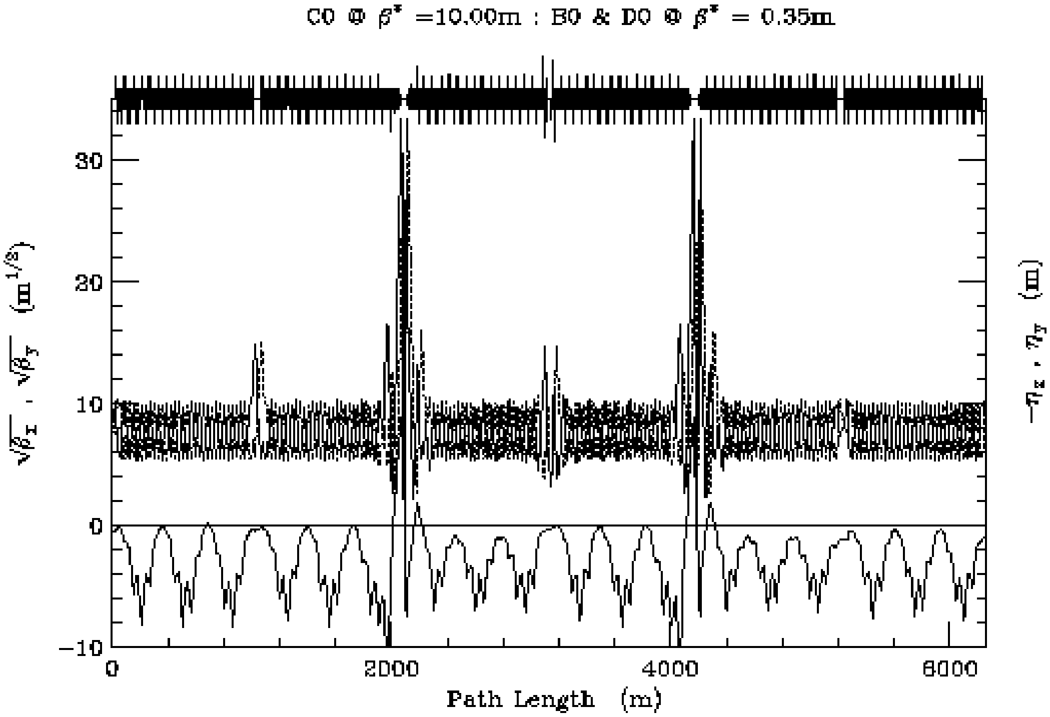

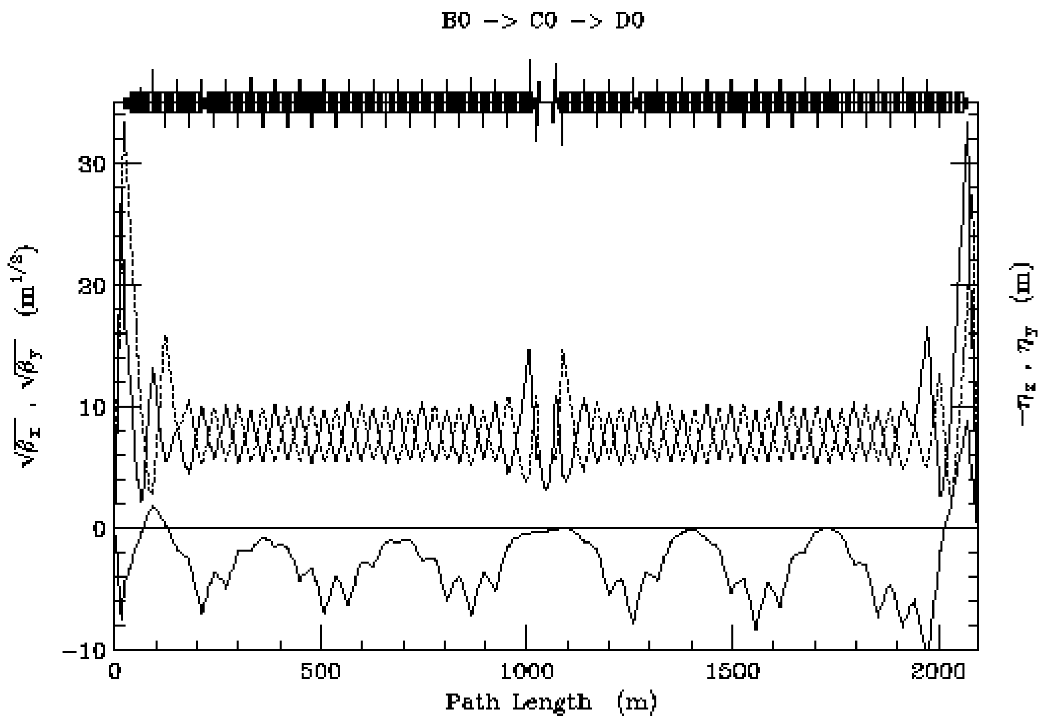

1 TeV Gradients for B0 & D0 @ Collision : Not C0

Quad #	C0 @ β^* = 10.00 m up	C0 @ β^* = 10.00 m down
Q1	3.755 kA	-3.755 kA
Q2	-4.236 kA	4.236 kA
Q3	4.641 kA	-4.641 kA
Q4	-1.800 kA	1.800 kA
TQ5	4.859 T/m	-5.107 T/m
TQ6	**8.911 T/m**	**-8.895 T/m**
TQ7	0	0
TQ8	-5.929 T/m	4.936 T/m
TQ9	0.171 T/m	-3.186 T/m

Quad #	B0 & D0 @ β^* = 0.35 m up (T/m)	B0 & D0 @ β^* = 0.35 m down (T/m)
Q4	139.976	-139.976
Q3	-138.173	138.173
Q2	139.976	-139.976
Q1		
Q5	-46.168	46.168
Q6	-104.715	104.715
T6	-4.601	
T7	47.569	-49.092
T8	-8.843	8.268
T9	-52.365	50.074
T0	-7.910	9.521
TB	-4.894	

QFA4 = –6.0665 T/m : (μ_x, μ_y) = (20.8167, 20.8167)

QDD1 = 4.1366 T/m :

- 9.186 T/m maximum for : TQ5, TQ6, TQ8, TQ9, & T6, T8, TB
- 58.268 T/m maximum for : T7, T9, T0

Optics for C0 @ Collision : Not B0 & D0

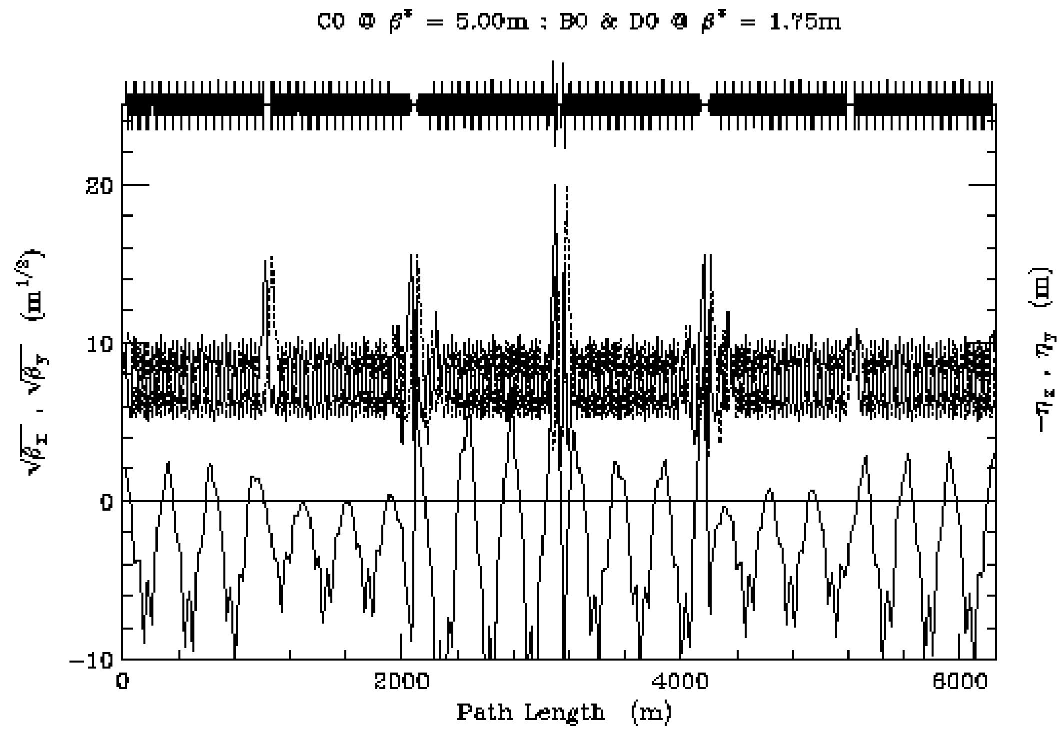

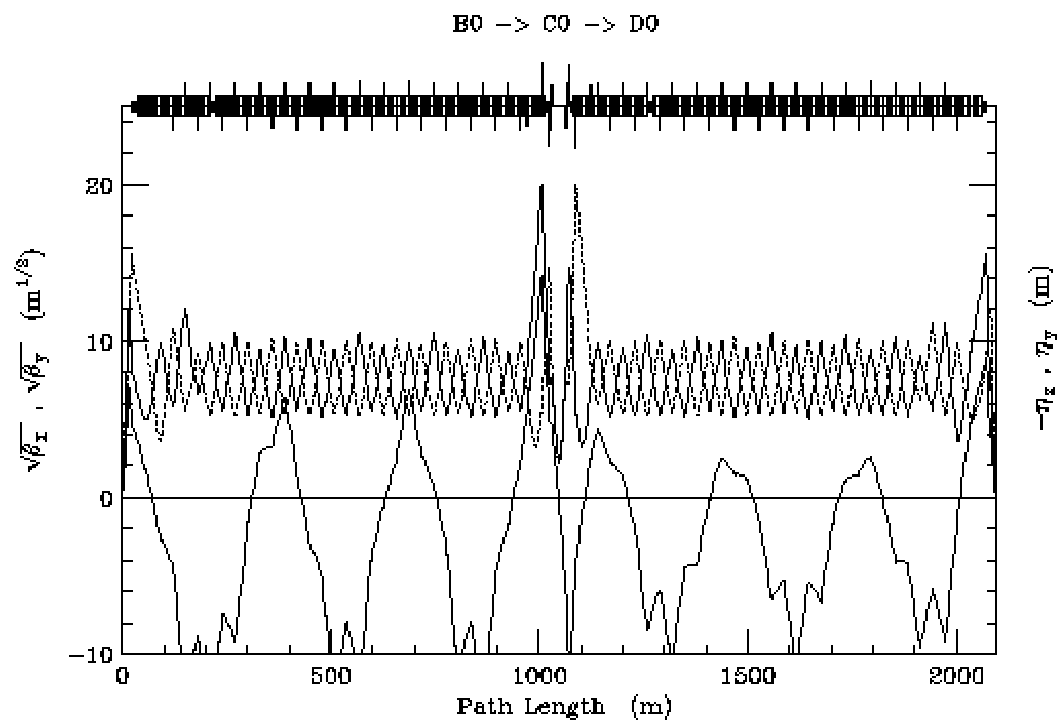

1 TeV Gradients for C0 @ Collision : Not B0 & D0

Quad #	C0 @ β^* = 5.00 m up	down
Q1	4.088 kA	-4.088 kA
Q2	-4.456 kA	4.456 kA
Q3	4.672 kA	-4.672 kA
Q4	-3.694 kA	3.694 kA
TQ5	-0.452 T/m	4.114 T/m
TQ6	-6.797 T/m	**8.819 T/m**
TQ7	0	0
TQ8	8.115 T/m	-1.855 T/m
TQ9	-1.051 T/m	4.482 T/m

Quad #	B0 & D0 @ β^* = 1.75 m up (T/m)	down (T/m)
Q4	132.025	-132.025
Q3	-133.147	133.147
Q2	132.025	-132.025
Q1		
Q5	29.528	47.181
Q6	0.624	107.324
T6	-6.359	
T7	42.061	-39.541
T8	3.185	**-8.819**
T9	-11.168	12.349
T0	13.366	-33.733
TB	6.038	

QFA4 = –0.5970 T/m : (μ_x, μ_y) = (20.8167, 20.8167)

QDD1 = –1.1017 T/m :

- 9.186 T/m maximum for : TQ5, TQ6, TQ8, TQ9, & T6, T8, TB
- 58.268 T/m maximum for : T7, T9, T0

Each of the solutions shown display similar characteristics:

(i) <u>All 3 IP's at Collision</u>:

(1) at C0 there is insufficient strength in the trim quads to match from dispersion in the arcs to $\eta^*=0$ at the IP. At the IP $\eta^* \approx 0.6$ m and $\eta'^* \neq 0$. At 1 TeV, for 30π emittance and σ_p/p = 0.85E-4, dispersion increases the horizontal beam size from $\sigma_X \approx 0.15$ mm to ≈ 0.16 mm.
(2) $\eta^* = 0$ at B0 & D0, but η'^* @ B0 = η'^* @ D0 = +0.57. Consequently, η reaches ~ 12 m in the B0 & D0 triplets, right where β also reaches its ring-wide maximum of ~1100 m. The beam size increases at this point from $\sigma \approx 2.25$ mm to ≈ 2.50 mm.
(3) $\eta > 10$ m in the arcs;
(4) β-wave ~±10 % in the arcs;

(ii) <u>Injection</u> :

(1) at the C0 IP dispersion is non-zero : $\eta^* \approx 1.3$ m and $\eta'^* \neq 0$;
(2) at B0 & D0 $\eta^* = 0$ but, again, $\eta'^* \neq 0$. η'^* @ B0 = –0.21, η'^* @ D0 = +0.21. η reaches ~ 8 m in the B0 & D0 triplets;
(3) $\eta > 10$ m in the arcs, and;
(4) β-wave ~±10 % in the arcs.

(iii) <u>B0 & D0 at collision : not C0</u> :

(1) at the C0 IP dispersion is non-zero : $\eta^* \approx 0.2$ m and $\eta'^* \neq 0$;
(2) at B0 & D0 $\eta^* = 0$, $\eta'^* \neq 0$. η'^* @ B0 = η'^* @ D0 = +0.46. η reaches ~ 9 m in the B0 & D0 triplets;
(3) $\eta > 8$ m in the arcs, and;
(4) β-wave ~±10 % in the arcs.

(iv) <u>C0 at collision : not B0 & D0</u> :

(1) at the C0 IP dispersion is non-zero : $\eta^* \approx 0.5$m and $\eta'^* \neq 0$;
(2) at B0 & D0 $\eta^* = 0$, $\eta'^* \neq 0$. η'^* @ B0 = –0.43, η'^* @ D0 = +0.43. η reaches ~ 9 m in the B0 & D0 triplets;
(3) $\eta > 14$ m in the arcs, and;
(4) β-wave ~±10 % in the arcs.

In each case some reduction in the value of η in the triplets is possible. This is only accomplished though by pushing 2 Bartelson trims plus 2 or 3 weak trims at each of B0 & D0, and an additional 3 or 4 trims at C0, to their maximum fields. Even in the solutions presented, the tables highlight that in several instances weak trims are already within 95 – 97% of their limits.

A striking feature to note in solutions (i) to (iv) is that, while the magnitude of $|\eta'^*|$ @ B0 = $|\eta'^*|$ @ D0, they are not necessarily the same sign. In conditions (i) & (iii) η'^* is positive at both IP's, whereas in (ii) & (iv) η'^* has opposite signs. So, for example, in making the transition from all 3 IP's at collision (i) to just C0 at collision (iv), at some point the B0 & D0 IR's are dispersion free, with $\eta^* = \eta'^* \equiv 0$. For the example cited this occurs at $\beta^* \approx 1.04$ m.

Sets of gradients exist that cover transitions among the 4 operating scenarios studied, but the solutions are very strained & 'unnatural'. At many stages during the transitions the trim quads at C0 & some trims plus Bartelson spools at B0 & D0 run near or at their maximum strengths. Even then, in some cases the arc β-wave grows beyond ±10%. The tables of gradients suggest that these difficulties should not be all that surprising – all 8 of the C0 matching trims change polarity at some point during transitions among the 4 operational conditions, and even the defocusing tune quad string QDD1 changes sign.

The failure to meet any of the listed optical requirements in any given operational scenario is directly related to the inability of the 8 tune quads to influence effectively the dispersion at the C0 IR – they are simply far too weak to produce the necessary phase advance. The result is a huge dispersion wave that, ultimately, the B0 & D0 trims must try to compensate, while still maintaining α, β matches.

The conclusions are disappointing, but should not be completely unexpected. The tune quads are more than 5 times weaker than Bartelson spools (7 T·m/m *cf* 37 T·m/m). Cynically, one could speculate that if 8 Bartelson spools are required for ideal matching, up to as many as 40 independent tune quads might be needed to obtain the same result!

4.2.1. Beam Separation

In Run II the Tevatron operates near the half-integer at ~20.5. From B0 → D0 is ~7.0, and in the long arc from D0 → B0 the tune is ~13.5. With this phase distribution, the separators upstream & downstream of the IP's are situated nearly ideally at collision. With zero crossing angle at B0, kicks from the B11 separators keep the beams separated up to C49, 180^{o} away in phase, where the kick is removed. Similarly, a kick at D11 can be removed 360^{o} away at A49. The additional arc separators contribute little to closing the 3-bumps. Adding a 3rd IR at C0, however, completely alters the nature of the problem of creating colliding beams at the IP's, but nowhere else.

The table below shows the phase advance from B0 → D0 and the locations of the separators. There is zero space elsewhere for more separators. With head-on collision at B0 & D0, a moment's reflection reveals that the B49 & C11 separators are largely irrelevant for beam control at C0. A kick at B11 can not be taken out ~90^{o} of phase away at B49, and just turns into a crossing angle at C0. This angle then propagates ~90^{o} downstream to C49, where it is canceled for head-on collisions at D0. It is not this simple in detail, of course, but it is apparent that the C0 separators play minimal roles.

* NAME	MUX	BETX	MUY	BETY
MB0	0.000000E+00	0.349987	0.000000E+00	0.349949
B11HESEP	0.248686	309.070	0.250270	1016.96
B11HESEP	0.250212	267.756	0.250724	919.044
B11VESEP	0.251984	229.458	0.251228	826.098
B17HESEP	1.14941	85.8618	0.854277	36.1764
B17HESEP	1.15480	77.0757	0.865723	40.7556
B17HESEP	1.16083	68.9509	0.875871	46.0047
B17HESEP	1.16758	61.4874	0.884861	51.9235
B49HESEP	3.53907	162.488	3.52488	122.166
B49VESEP	3.54330	100.836	3.52861	172.698
MC0	3.77769	5.00019	3.74521	5.00070
C11HESEP	3.99489	162.486	3.98056	111.342
C11VESEP	3.99801	122.180	3.98382	162.473
C17VESEP	4.80453	88.7063	4.47095	35.5010
C17VESEP	4.80975	79.7938	4.48259	40.1816
C17VESEP	4.81556	71.5340	4.49286	45.5555
C17VESEP	4.82206	63.9270	4.50192	51.6228
C49HESEP	7.28053	805.322	7.25625	221.095
C49VESEP	7.28105	897.114	7.25809	258.703
C49VESEP	7.28152	993.877	7.25967	299.327
MD0	7.53188	0.349987	7.50868	0.349949

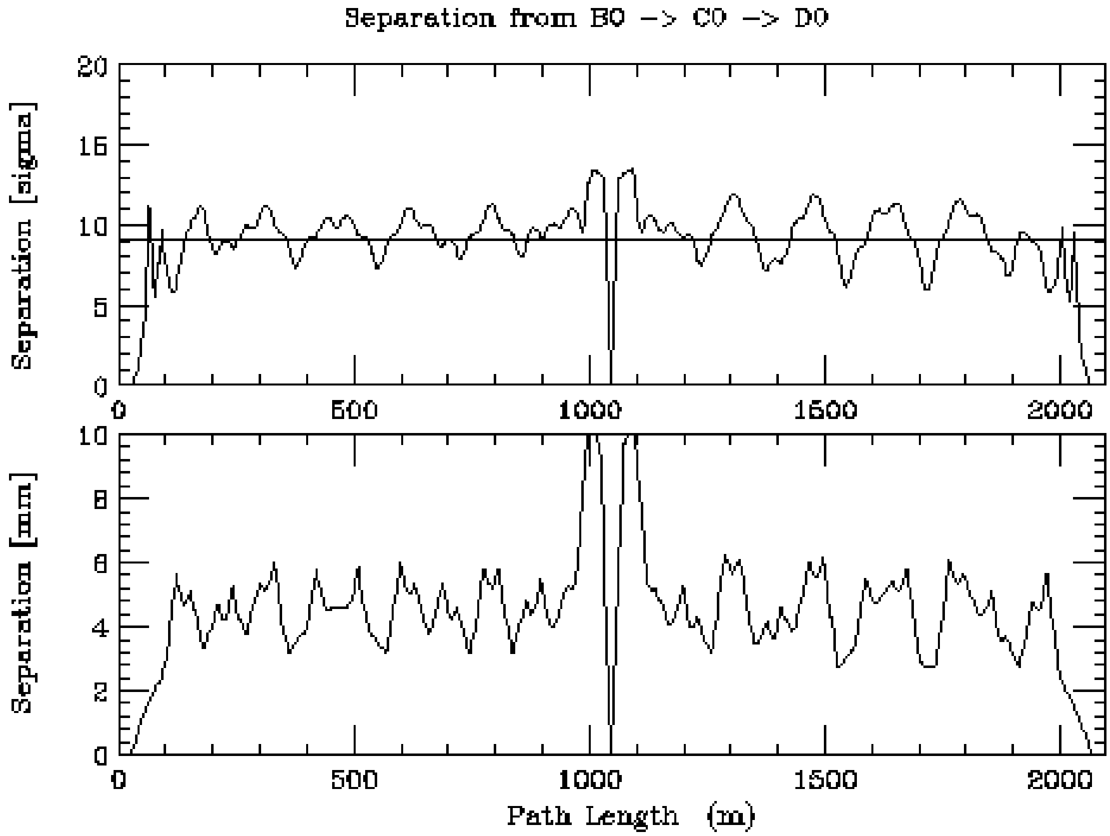

Gradients:

B11H (2) :	+4.0000 MV/m	B11V(1) :	-4.0000 MV/m
B17H (4) :	-0.8113		
B49H (1) :	+0.3956	B49V(1) :	+0.3480
C11H (1):	-0.1624	C11V(1) :	-0.3480
		C17V(4) :	-0.5526
C49H (1) :	-4.0000	C49V(2) :	+3.4918

The preceding example shows one possible solution for creating separated beams in the short arc during collision. The plot shows beam separation in both sigmas of separation (for a 30π beam) & mm's of separation. The corresponding separator gradients are listed in the accompanying table. As noted earlier, most of the beam control comes from the B11 & C49 separators, with the others contributing little. The average beam separation here is 9.0 sigma across the arc, and at C0 there are half-crossing angles of $\alpha_x = -\alpha_y = 133$ μr -- for a total half-crossing angle of 188 μr.

The following table lists the phase advance through the long arc D0→E0→F0→A0→B0. Existing separators are indicated, together with all spaces where new separators could be installed.

* NAME		MUX	BETX	MUY	BETY
MD0		0.000000E+00	0.350001	0.000000E+00	0.350002
D11HESEP		0.249021	299.282	0.250360	993.834
D11HESEP		0.250599	258.664	0.250825	897.076
D11VESEP		0.252436	221.062	0.251342	805.288
MD17		1.13913	97.1271	0.824092	31.5623
DD17SP2	264.25"	1.15443	77.6316	0.865017	40.4301
D48HESEP		3.50765	98.0203	3.21588	30.4788
ME0		3.63534	67.3049	3.38148	71.7560
DE0SP7	330.55"	3.66736	84.8937	3.41840	60.2007
ME17		4.27783	94.0859	3.95889	30.1939
DE17A	164.75"	4.28931	81.2037	3.99223	35.1224
DE17B	128.125"	4.29715	70.3793	4.00784	41.0775
DE17C	72.75"	4.30322	63.6144	4.01720	45.8535
DE17D	93.125"	4.30872	58.4325	4.02419	50.2216
DA0SP5	257.20"	9.84087	128.649	9.69882	69.2994
MA0		9.85416	93.5980	9.71634	99.9831
DA0SP11	340.30"	9.87531	62.9429	9.72990	143.065
ESEP	101.25"	10.5574	88.7032	10.2703	35.5048
ESEP	101.25"	10.5627	79.7911	10.2819	40.1865
ESEP	101.25"	10.5685	71.5318	10.2922	45.5617
A17VESEP		10.5750	63.9252	10.3012	51.6303
A49HESEP		13.0336	825.973	13.0560	229.449
A49VESEP		13.0341	918.905	13.0578	267.745
A49VESEP		13.0345	1016.81	13.0593	309.057
MB0		13.2848	0.350001	13.3080	0.350002

Whereas in the Run II lattice there is an integer number of wavelengths between the D11 & A49 separators, there is now ~270^{o} of phase separation. This is as bad as it can possibly get – a kick at D11 turns into a pure displacement at A49. As a result, the orbit can no longer be closed using just 3-bumps in the horizontal & vertical planes -- 4-bumps, at least, are required.

From the table, one option in the vertical plane is to add additional separators to the E17 drifts. By shifting around the pinger & flying wire at E17, it should be possible to stuff in 3 separators. There are then 2 clear 3-bumps to close the orbit vertically: D11 - E17 - A17 and E17 - A17 - A49. It is not nearly so clear what to do horizontally though. The closest there are to simple 3-bumps are: D11 - D48 - A0 and D48 - A0 - A49. At A0 there should be room to squeeze 5 separators in with the 5 proton abort kickers, 5 pbar abort kickers, collimator & 2 abort blocks.

Shown below is one possible orbit solution using these 4-bumps, followed by the corresponding gradients. The average beam separation is 9.4 sigma. While the beams do stay well apart through most of the arc, separation falls apart badly in A-sector.

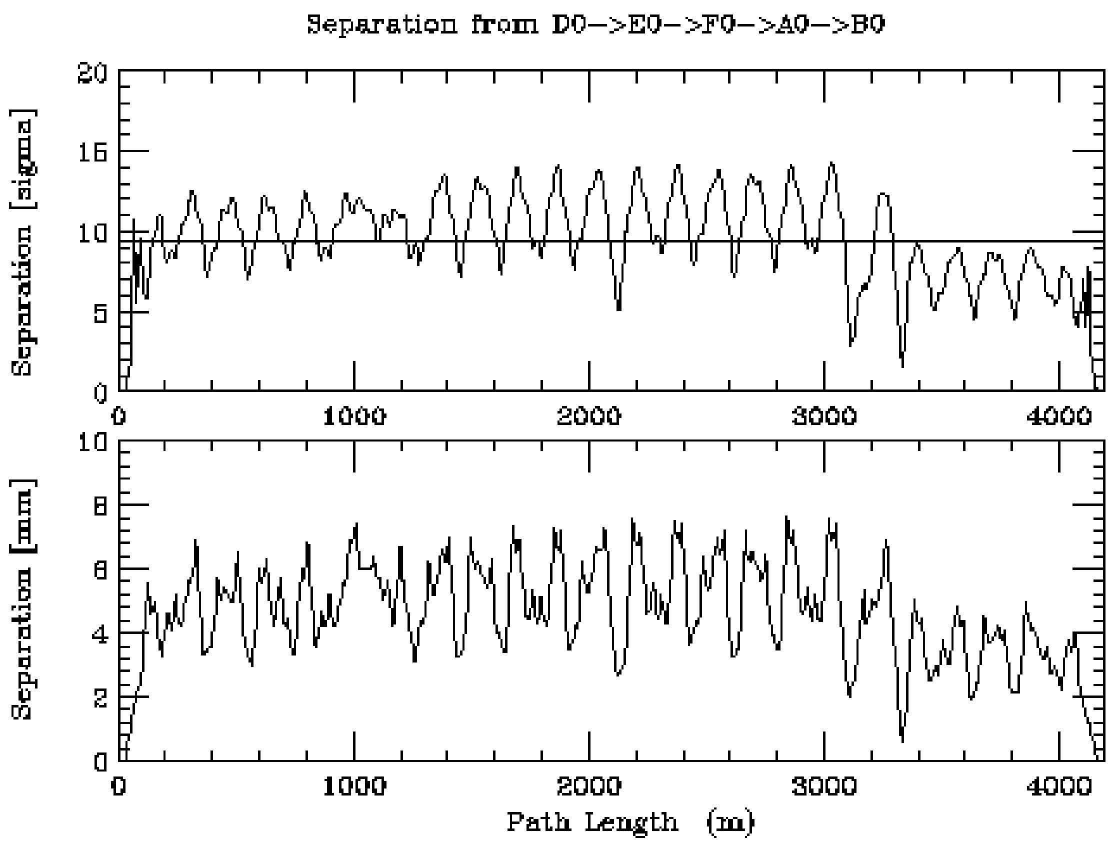

Gradients:

D11H (2) :	+4.0000 MV/m	D11V(1) :	-4.0000 MV/m
D48H (1) :	+3.5374		
		E17V(3) :	-3.1035
A0H(5):	+4.0000		
		A17V(4) :	-3.1035
A49H (1) :	-2.8577	A49V(2) :	-2.8032

Note that at A0 & E17 all available separator space is consumed, while at A17 the number of vertical separators increases from 1 to 4. There are certainly other solutions using this separator configuration, and a number of alternate combinations of separator locations that can be explored. None pursued in this study, however, looked appreciably better than the result given here – they're just bad in different places.

4.3. Summary

With Bartelson-like trim quad spools it is possible to satisfy most of the optics restrictions imposed on the IR design. These magnets do not currently exist though & would require a serious commitment of time and money to construct. With the much weaker regular quad spools for matching, a partial optical & partial separator solution has been patched together for a C0 IR insert. It meets none of the 10 original design constraints however, other than it is constructed solely from existing magnets.

With the completely disrupted betatron phase distribution around the ring that results from adding a 3rd IR, the existing separators are no longer in optimum locations. Creating acceptable collision helices becomes very difficult & requires many additional new separators.

5. MEDIUM–β^* SUMMARY

It does not appear possible to create an IR insert at C0 using just the existing Tevatron spare magnets. The design efforts presented here illustrate some of the inherent difficulties of this task:

- There is insufficient room in the straight to accommodate the final focus magnets plus the necessary number of separators. The limited space, coupled with the low gradients of the magnets compared to the B0 & D0 triplet quadrupoles, determines that the final focus must be a doublet. The space remaining after the doublet is installed can hold, at most, just 2 separators, rather than the desired number of four. With the relatively small values of β at the separators, it is difficult to produce adequate beam separation in the arcs.

- Matching from the IP optics into the standard arc lattice functions is accomplished through two, equally unacceptable, approaches:

    (i) Independent powering and/or replacing arc magnets to achieve optical matching results in the spool pieces being eliminated at those locations. The necessary correction elements are therefore lost and, possibly, the BPM's as well.

(ii) Using just 8 of the spool quadrupole components for the final match to the arcs reveals that the quads require gradients several times stronger than they are capable of reaching. These spools would therefore have to be replaced with new magnets, such as the Bartelson spools used at B0 & D0.

- Powering just 8 of the weak tune quads individually ends any hope of making an ideal optics match to the arc. The result is havoc in the lattice functions around the ring & disruption of normal operating conditions at the other detectors. Characteristic traits of this solution are:

  (i) $\eta^* \neq 0$ & $\eta'^* \neq 0$ at the C0 IP;
  (ii) $\eta'^* \neq 0$ at the B0 & D0 IP's;
  (iii) $\eta > 9$ m in the B0 & D0 triplets;
  (iv) $\eta > 10$ m in the arcs, and;
  (v) β-wave ~±10 % in the arcs.

- Creating adequately separated orbits in the arcs while maintaining head-on collisions at B0 & D0 is hard. The addition of the 3rd IR, and subsequent tune re-adjustment, redistributes the betatron phase around the Tevatron. Existing separators are no longer in the optimum locations for beam control & many new separators are required. Although not studied for this report, the phase changes also affect the operation and/or placement of correction schemes, collimators, feed-down circuits, etc.

This study does not pretend to exhaust all conceivable C0 inserts -- other design ideas could certainly be pursued. <u>Any</u> insert, however, will confront many of the same difficulties discovered here, and must also address issues related to the overall impact of a C0 IR insert on Tevatron operations.

6. HIGH–β^* C0 IR

With the failure to find a viable medium–β^* solution, this section explores possibilities for creating colliding beams at C0 with high–β^* optics. Section 6.1 looks at modifying the Collins insert optics slightly to install separators in the C0 straight for additional beam control. Section 6.2 considers C0 collisions with no lattice modifications.

6.1. Modified Collins Insert

The standard Collins insert at C0 (shown below) can be altered to accommodate 2 separators up & downstream of the IP, while maintaining an optical match to the arc lattice functions. The 32", 82", & 99" inner quads of the standard insert are replaced with 25", 66", & 82" quads, respectively. The inner 82" quads move in towards the C0 interaction point sufficiently to insert 2 separators between the 66" & 82" quads. These replacement magnets continue to run on the main bus.

Layout of the modified C0 region and optical functions appear on the following page. In this new configuration β^* at C0 grows from the standard Collins value of ~72 m up to ~ 82 m, while at the separators $\beta_X \sim \beta_Y \sim$ 90-105 m.

STANDARD COLLINS C0 STRAIGHT

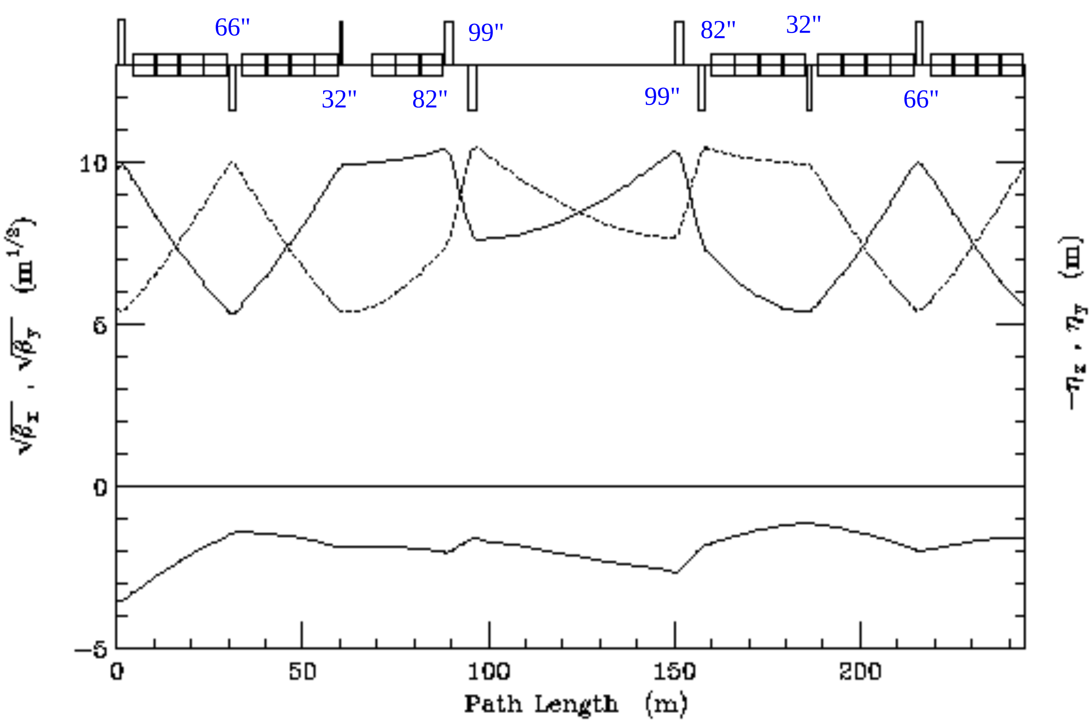

MODIFIED C0 OPTICS

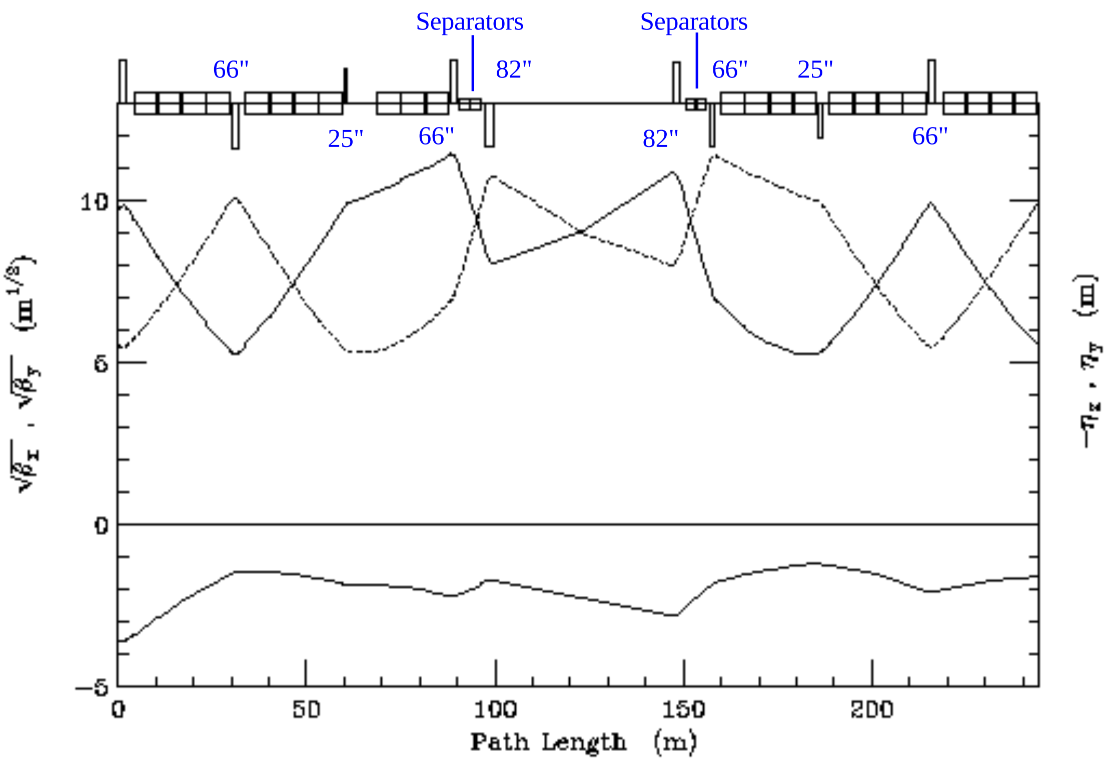

B0 -> D0 with Modified C0 Insert & ß* = 0.35m @ B0 & D0

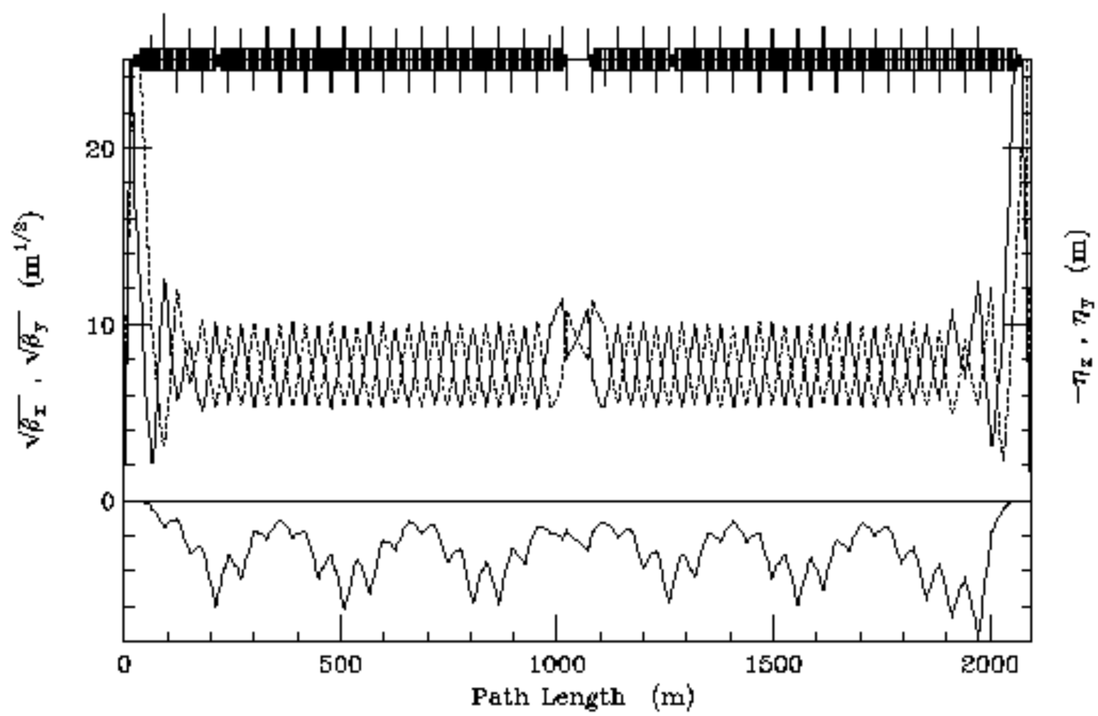

6.1.1. Colliding Beams

It is <u>not</u> possible to create collisions at all 3 detectors, with or without a crossing angle at C0. The following table lists the betatron phase advance from B0 $\rightarrow$ D0, indicating the locations of separators. There is zero space elsewhere in the short arc to fit additional separators.

* SHORT ARC OPTICS FROM B0 -> D0 WITH BOGUS C0 INSERT

* NAME	BETX	MUX	BETY	MUY
MB0	0.350514	0.000000E+00	0.348948	0.000000E+00
B11HESEP	311.267	0.251237	1021.70	0.251281
B11HESEP	270.806	0.252750	924.065	0.251733
B11VESEP	233.214	0.254497	831.350	0.252234
B17HESEP	84.4476	1.10674	34.2864	0.846182
B17HESEP	75.5902	1.11224	38.8140	0.858231
B17HESEP	67.4139	1.11839	44.0402	0.868860
B17HESEP	59.9189	1.12530	49.9651	0.878226
B49HESEP	108.449	3.57646	67.0730	3.38192
B49VESEP	88.4504	3.58095	86.6243	3.38768
MC0	81.4232	3.64463	81.7756	3.43410
C11HESEP	86.2665	3.69125	88.6553	3.49756
C11VESEP	66.8043	3.69704	108.677	3.50204
C17VESEP	82.6681	4.31727	34.6247	4.03513
C17VESEP	73.9726	4.32288	39.2903	4.04704
C17VESEP	65.9550	4.32917	44.6639	4.05753
C17VESEP	58.6152	4.33624	50.7457	4.06676
C49HESEP	806.957	6.82195	225.776	6.83672
C49VESEP	898.247	6.82247	262.976	6.83852
C49VESEP	994.445	6.82293	303.074	6.84007
MD0	0.350514	7.07072	0.348948	7.08805

Kicks from the B11 separators in each plane translate into nearly pure displacements at C0, and then back into angles downstream at C49, where they are canceled. The B17 horizontal separators are roughly 180^{o} upstream of C0, so that B17 kicks manifest predominantly as crossing angles at C0, with little affect on position. In the vertical plane there are no existing separators between C11 & the newly added B49 separators.

The separators added at B49 & C11 are of limited value. Due to the uniformly large value of β across the insert, the phase difference between the separators & the C0 midpoint is only ~2π·(0.05). This is woefully inadequate for any significant position control at the IP. To produce x=y=0 at the interaction point requires ~22 MV/m/separator -- nearly 6x what is physically realizable. With a maximum kick of only ~10 μr/separator available at 1 TeV, there is very little in the way of crossing-angle control either.

MODIFIED C0 COLLINS INSERT

B49 H&V = -4.00 MV/m   : C11 H&V = -4.00 MV/m

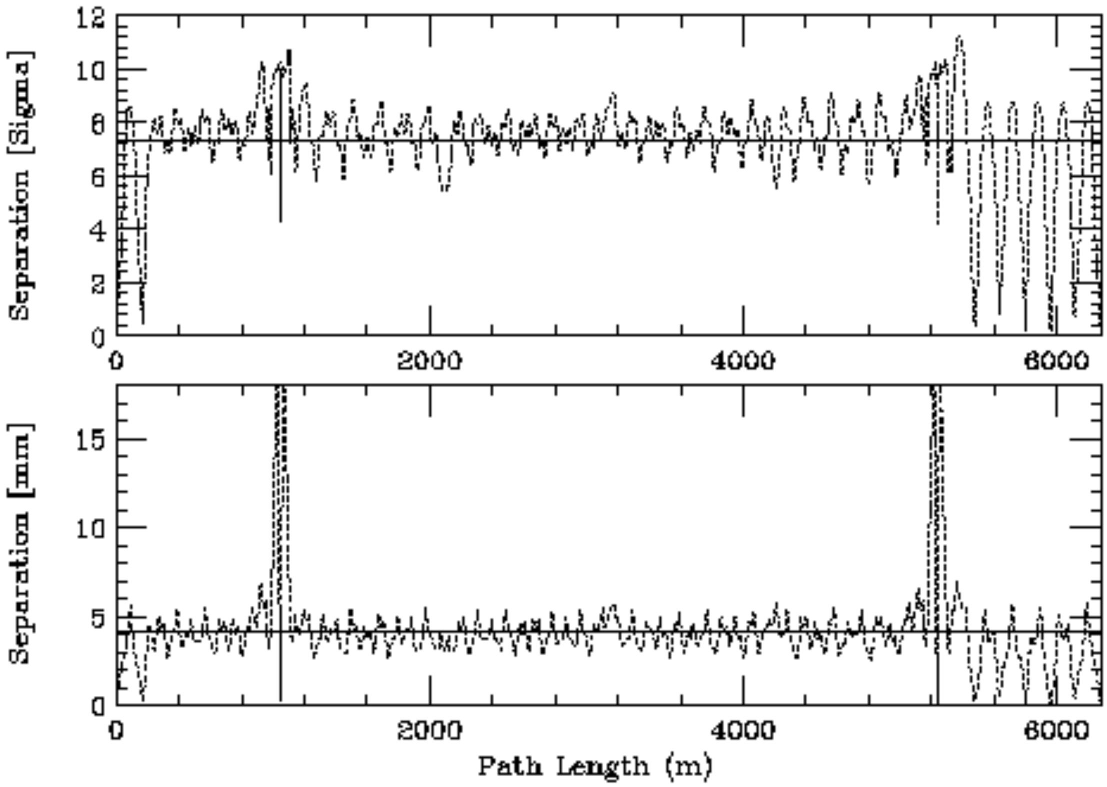

Gradients:

		B11V(1) :	+2.8960 MV/m
B17H (4) :	+4.0000 MV/m		
B49H (1):	−4.0000	B49V (1):	−4.0000
C11H (1):	−4.0000	C11V (1):	−4.0000
		C17V(4) :	+4.0000
C49H (1) :	+0.1046		

The preceding is an illustration of creating collisions at C0, while separating the beams elsewhere in the ring. In this example (chosen rather arbitrarily), B0 & D0 have $\beta^* = 35$ cm. The corresponding separator gradients appear in the accompanying table.

The average beam separation here is 7.2 sigma around the ring, with half-crossing angles of $\alpha_x = -\alpha_y = 21$ μr at C0; for a total half-crossing angle of 30 μr. The beams are separated adequately through most of the machine, but fall together badly through B–sector.

6.2. Standard Collins Straight

In the middle of the regular C0 straight section $\beta_x \approx \beta_y \approx 71$ m and $\alpha_x \approx -\alpha_y \approx \pm 0.47$. Between the 99" & 82" innermost quads at the ends of the straight (where $\sqrt{\beta_x} \approx \sqrt{\beta_y}$) there is insufficient room for separators.

6.2.1. Colliding Beams

The observations in the preceding section regarding phase advances from place-to-place in the ring apply equally to the unaltered C0 Collins insert. With the same operating example as considered in section 6.1 ($\beta^* = 35$ cm @ B0 & D0), the beams can again be brought into collision at C0 using just the B17 & C49 horizontal and B11 & C17 vertical separators. Gradients are given in the following table, and the beam separation is shown on the following page.

<u>Gradients</u>:

		B11V(1) :	+2.7810 MV/m
B17H (4) :	+4.0000 MV/m		
		C17V(4) :	+4.0000
C49H (1) :	+0.0655		

The orbits have similar characteristics to those found with the modified Collins insert & separators at B49 & C11. The average beam separation is 5.8 sigma around the ring, which is somewhat less than before. Again, though, the beams are fairly well separated through much of the machine, but fall together badly through B–sector. At C0 there are half-crossing angles of $\alpha_x = -\alpha_y = 21$ μr, for a total half-crossing angle of 30 μr.

STANDARD C0 COLLINS INSERT

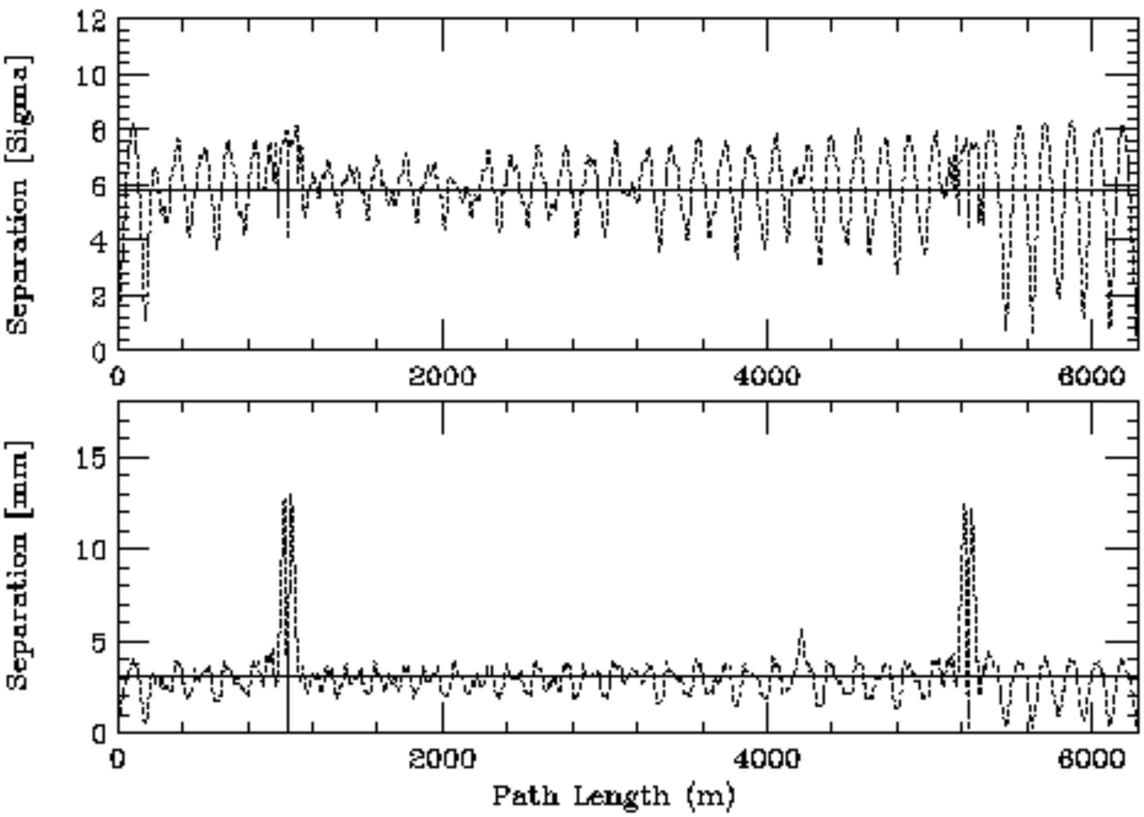

6.3. Summary

Since collisions can not occur at all 3 IP's simultaneously, colliding beams at C0 must be created during some kind of dedicated Tevatron operation. While it is possible to install separators at C0 after modifying the Collins insert, it is certainly not obvious that the effort is worthwhile. In the example described, C0 collisions can be created with or without new C0 separators. The B49 & C11 separators did improve beam separation somewhat through the arcs but, in either case, separation was very poor in B-sector. Definitive conclusions regarding C0 modifications will only become possible after realistic operational scenarios have been studied.

7. CONCLUSIONS

No successful design was found for a C0 medium–β^* IR insert that could be constructed solely from existing magnets. Failure of the attempts reported were a result of 2 factors: (a) insufficient space exists for installation of the required components, and; (b) the optical impact on the Tevatron would completely disrupt normal machine operations.

If a positive side to this study exists, it is that several stumbling blocks were identified that will have to be addressed eventually by <u>any</u> low–β^* design. The 2 most important are the following:

- The BTeV detector reduces the available free space by ~20' each side of the IP compared to B0 & D0. So, a final focus modeled on the B0 & D0 high-gradient triplets plus separators would not fit in the C0 straight. Furthermore, it is very unlikely that a triplet would fit even if constructed using higher gradient (LHC) magnets. There are two options as to how to proceed:

    (i) The final focus is constructed as a high-gradient doublet. This creates sufficient space to install the optimum number of 4 separators. However, the β^* attainable for collisions is then severely limited by the available aperture in the quadrupoles. The studies reported here showed that with a doublet, a $\beta^* \approx 1$ m results in $\beta_{max} \approx$ 1500 m. This is <u>not</u> a problem that goes away with higher gradients!

    (ii) The final focus is a high-gradient triplet, producing collisions at $\beta^* \leq 35$ cm. Installing the 3 separators requires creating new space into the arcs. In this scenario the inventory of new IR magnets therefore also includes high-field dipoles.

- A 3rd IR in the Tevatron adds roughly a half-integer of tune to the machine. If re-tuning is distributed over the entire ring, none of the correction elements, separators, collimators, etc., are in the appropriate locations any longer. Every aspect of machine operations must then be re-evaluated. This study emphasized that the optimum choice for tune re-adjustment is to confine it to the short arc, adding or subtracting ~90^o between B11 & B49 and again between C11 & C49. This has minimal impact on normal operations & appears to be the only way to create head-on collisions at all 3 IP's simultaneously. However, this is not possible with the current weak tune quad strings & 'some' number of additional strong tune quads are required.

Creating a low–β^* insert for C0 appears to be a real challenge. To be compatible with other aspects of Tevatron operations, the enhanced list of IR magnets required indicates this will be a significantly larger undertaking than was construction of the 2 existing IR's.

A I : Spare Quadrupoles

Quad ID	Quench Test (A)	Cycle Test (A)	Location
N9925F	4301	4332	B49 - 1Q
N9931F	4989	4887	C11 - 0Q
N9909F	4850	4694	MSB
N9921F	5050	4738	MSB
H9003F	5303	4972	MSB
H9004D	4989	4875	MSB
H8211F	4518	4324	B49 - 1
H8214D	4501	4383	C11 - 1
H8202D	4767	4594	MSB
H8207F	5342	4900	MSB
TQ216	4363	4556	B47 - 1
TQ237	4683	4603	C13 - 1
TQ050	4991	4745	MSB
TQ057	4989	4769	MSB
TQ103	4963	4956	MSB
TQ117	4867	4845	MSB
TQ121	4998	4756	MSB
TQ127	4989	4804	MSB
TQ169	4998	4853	MSB
TQ245	5717	5443	MSB
H3215F	4859	4695	B48 - 1
V3206D	4898	4481	C12 - 1
V3208D	4825	4984	MSB
H3211F	4952	4811	MSB
V2502D	4716	4551	MSB
H2507F	4906	4753	MSB
N5417F	5175	-100	A49 - 1
N5419F	5171	5088	B11 - 1

A II : Tune Space from 20.5 $\rightarrow$ 20.9

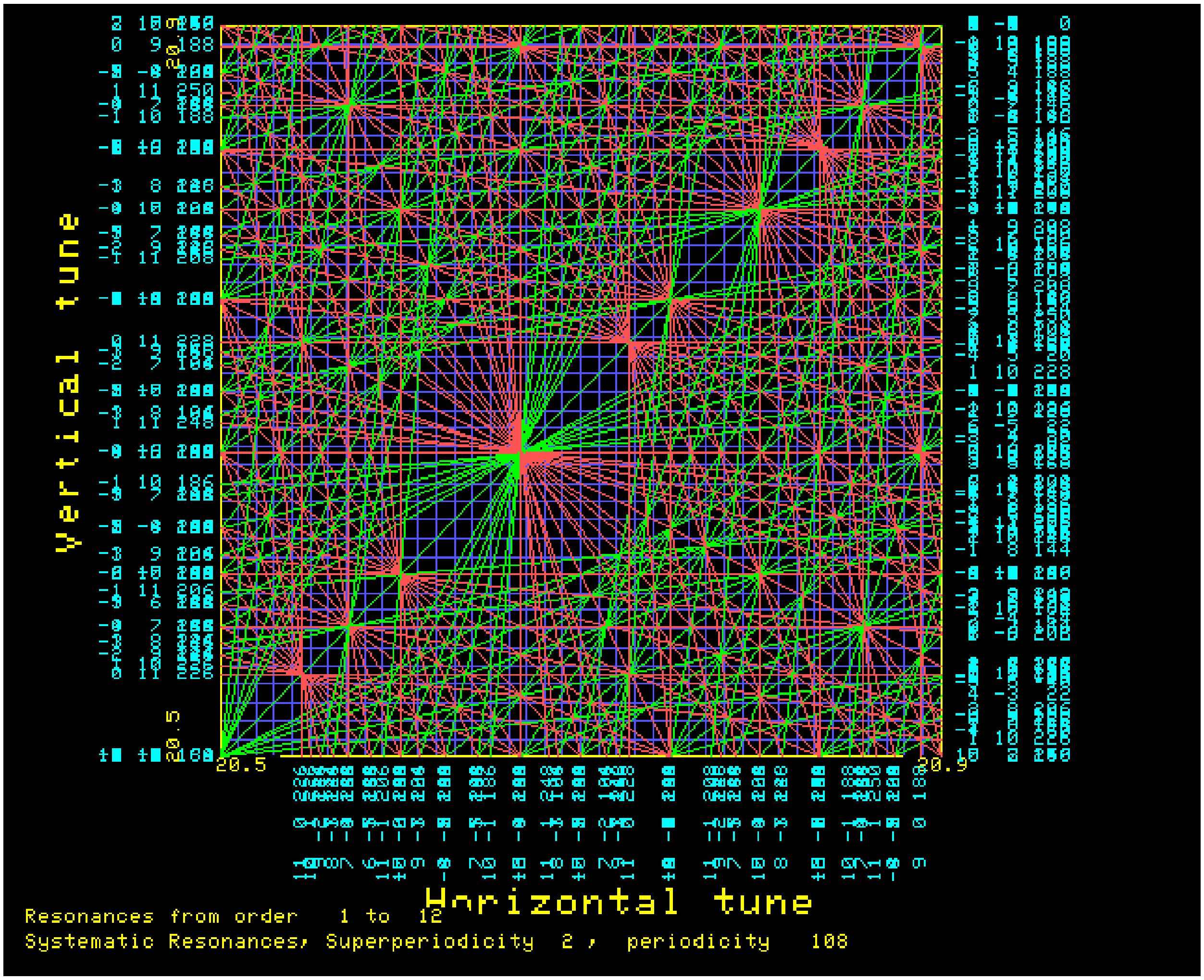

A III : The Bed of Nails

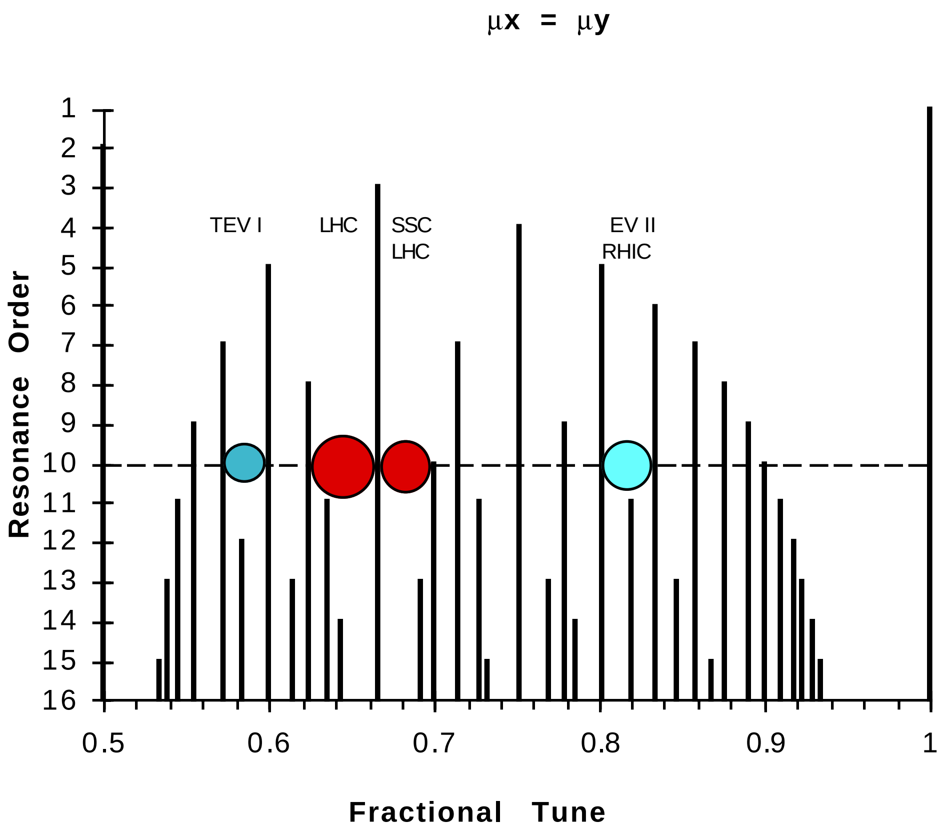

- Consider tunes near the diagonal.
- Avoid resonances at least up through 10th order, as illustrated in the "Bed of Nails" resonance diagram.
- For the Run I & II lattices ("TeV I" in the diagram) the separation between the $^4/_7$ & $^3/_5$ resonances is $\Delta\mu$ = .0286
- Large sextupole components in the magnets precludes operating the Tevatron at the LHC & SSC operating points.
- For running with 3 IP's choose between the $^4/_5$ & $^5/_6$ resonances, at .8167; the same fractional tune as RHIC. For "TeV II" $\Delta\mu$ = .0333, which is wider than the original "TeV I".

A IV : Layout of C0 IR $^{\lambda}/_4$ Transformer

The complete layout of the C0 IR from B47 -> C13 is illustrated on the following 2 pages. Clearly the notion of 'scale' is a very fluid concept in these pictures, and the diagrams are intended only to document distances, dimensions, & relative positions of the major components plus their ancillary hardware.

Dipoles & separators depicted in the drawings are defined by the 2 entities below.

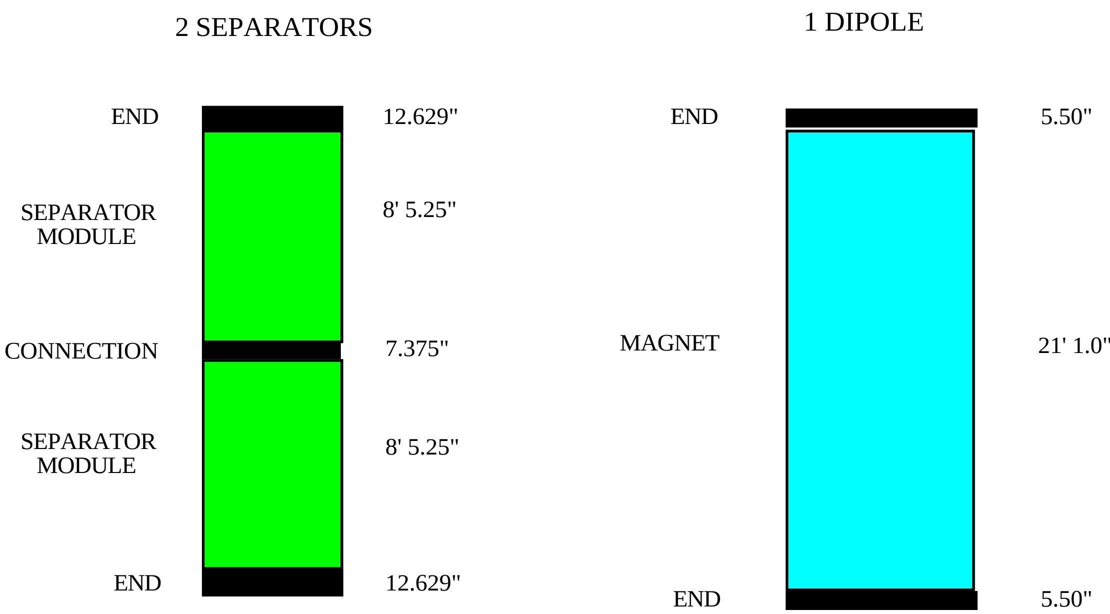

IV.a. Upstream C0

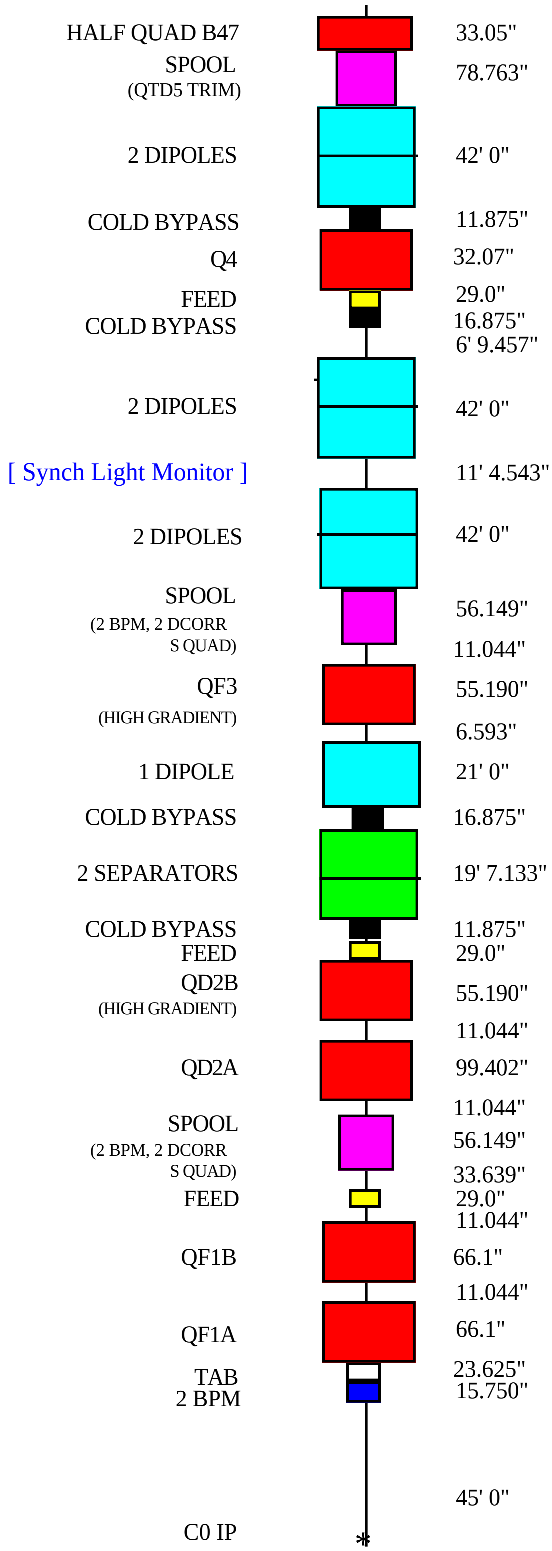

IV.b. Downstream C0